STUDIES OF ELECTRONIC COMMUNICATION BETWEEN

DIMOLYBDENUM CORES JOINED BY VARIOUS BRIDGES

A Thesis

by

JIAYI JIN

Submitted to the Office of Graduate Studies of
Texas A&M University
in partial fulfillment of the requirements for the degree of

MASTER OF SCIENCE

August 2007

Major Subject: Chemistry

STUDIES OF ELECTRONIC COMMUNICATION BETWEEN

DIMOLYBDENUM CORES JOINED BY VARIOUS BRIDGES

A Thesis

by

JIAYI JIN

Submitted to the Office of Graduate Studies of
Texas A&M University
in partial fulfillment of the requirements for the degree of

MASTER OF SCIENCE

Approved by:

Co-Chairs of Committee,	Carlos A. Murillo
	John P. Fackler, Jr.
Committee Member,	Donald G. Naugle
Head of Department,	David H. Russell

August 2007

Major Subject: Chemistry

ABSTRACT

Studies of Electronic Communication between Dimolybdenum Cores Joined by Various

Bridges. (August 2007)

Jiayi Jin, B.S., University of Science and Technology of China

Co-Chairs of Advisory Committee: Dr. C. A. Murillo
Dr. J. P. Fackler, Jr.

A series of metal-organic complexes which all contain two bridged dimolybdenum cores were synthesized and studied. Common building blocks involved in this series of syntheses include $Mo_2(DAniF)_3(O_2CCH_3)$ (DAniF = *N*, *N'*-di-*p*-anisylformamidinate) and $[Mo_2(cis-DAniF)_2(NCCH_3)_4](BF_4)_2$. Bridges that were used to connect two different dimolybdenum cores in the synthesized structures include single metal complexes like $ZnCl_2$ and $Ni(acac)_2$ (acac = acetyl acetone), dimetal complex like $Rh_2(O_2CCH_3)_4$, as well as organic ligands like 1,2-dihydroxyl-4,5-dimethylaminbenzene and 1,3-dihydroxyl-2,5-dimethylaminbenzene.

Several heterometallic supramolecules were obtained through self-assembly reactions. In these structures, the two dimolybdenum cores were bridged through different metal complexes; between these metal complexes and the molybdenum cores, isonicotinic acid anion acts as the key linkage. Depending on the geometry of the building blocks and their available binding site, these heterometallic supramolecules bear a variety of shapes, which include rod-like molecules with three metal centers, a square-shaped molecule with its four corners occupied by metal complexes, and also a zigzag-shaped infinite metal complex chain. Although these molecules do show reversible redox peaks in electrochemistry studies, they demonstrated very poor electronic communication

between the dimolybdenum centers. Possible explanations to this result may be that the dimolybdenum cores are far away from each other in these molecules (Mo$_2$–Mo$_2$ separation in compound **4**, being 21 Å, is the longest among all dimolybdenum pairs synthesized to date) and that the calculated frontier orbital overlaps do not favor electron delocalization over the entire molecule.

However, another type of molybdenum dimer of dimers where the dimolybdenum centers are united by conjugated organic ligands, namely 1,2-dihydroxyl-4,5-dimethylaminbenzene and 1,3-dihydroxyl-2,5-dimethylaminbenzene, were also synthesized and found to bear significantly stronger electronic communication between the Mo$_2$ centers.   In fact, as electrochemistry reveals, these molecules demonstrated the greatest comproportionation constant values ($K_c \sim 10^{14}$) than any other analogues synthesized so far. This interesting result is most likely due to the well conjugated linker ligands that would allow electrons on the metal centers to delocalize over the entire molecule. Computational studies of these compounds also show clear evidence of π overlapping in their molecular frontier orbitals.

DEDICATION

I dedicate this work to

The memory of my graduate research advisor Professor F. A. Cotton

My beloved mother, Yinna Xu, father, Shuigen Jin, and brother, Jiaming Jin

ACKNOWLEDGEMENTS

TABLE OF CONTENTS

LIST OF TABLES

LIST OF FIGURES

CHAPTER I

INTRODUCTION

Electronic interaction between two or more adjacent metal centers joined by various linkers[1] has long been an interesting topic for chemists, especially in the area of inorganic chemistry. The earliest systematically studied example of this topic is the pyrazine-bridged Ru dimer, $\{[Ru(NH_3)_5](pyz)[Ru(NH_3)_5]\}^{5+}$ (**I** in Figure 1), which is also known as the Creutz-Taube (C-T) ion.[2] The C-T ion has been used as a prototype for hundreds of compounds to solve the issues including the location of the odd electron in compounds of this type, the extent of the electronic communication between the two metal centers mediated by the linkers, and the pathway of electron transfer from one end (donor) to the other (acceptor).

I
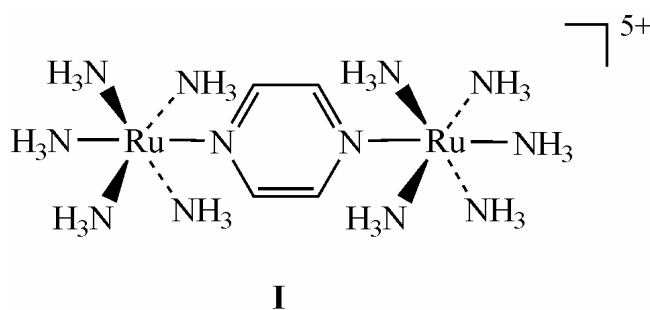
Figure 1. The Creutz-Taube (C-T) ion.

Ever since the late 1960's, the time when the C-T ion was synthesized and studied, a large number of similar systems has been synthesized and investigated.[3, 2] This system, which was normally recognized as a class of inorganic compounds containing

---

This thesis follows the style of *Inorganic Chemistry*.

two or more metal atoms of the same elements but in different formal oxidation states, was named mixed-valence (MV) system. The concept of mixed-valence chemistry is of significance in a variety of interdisciplinary areas for many reasons, which include that 1) it augments the fundamental knowledge of chemistry, 2) it help chemists search for a better understanding of important biochemical redox and electron transfer process, and 3) it promotes the idea of fabrication of nanoscale structures in materials science.[4] More recently MV systems have been of interest for the development of highly conducting materials, energy storage devices and molecular electronic applications, for example, molecular wires and molecular switches.[5]

Various chemical and physical methods such as X-ray structure analysis, electrochemical studies, spectroscopic and magnetic measurements have been used to probe the electronic communication between metal centers in MV systems. Depending on the ability of the linker to conduct electrons from the electron donating center to the electron accepting center, mixed valence systems have conventionally been divided into three classes in the widely accepted Robin-Day categories,[6] that is, Class I (no interaction, localized valency), Class II (weak to medium coupling, valence trapped), and Class III (strong interaction, delocalized). Earlier work by Hush[7] illustrated the three Classes of mixed valence compounds by a classical potential energy configuration diagram shown in Figure 2, in which the X axis is a coordinate expressing the Ru_a^{III}-N distance as the sum of Ru_a-N and Ru_b-N is held constant. The systems vary from completely localized systems (Class I) to intermediate (Class II) to completely delocalized (Class III). For Class I and Class II compounds, there are two potential energy minima and the odd electron is energetically favored to be localized, with equal

probability on each metal center because of large energy barrier (E_{th}) for thermal electron transfer, whereas in Class III compounds, due to the strong electron coupling, this energy barrier is not present, $E_{th} = 0$, and the odd electron is present actually equally on both metal centers which are indistinguishable.
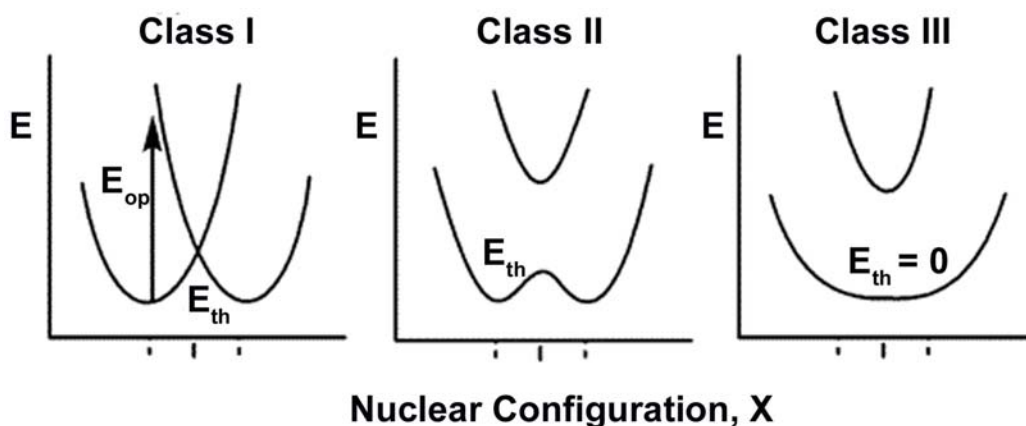
Figure 2. Potential energy configuration curves for the three classes of mixed valence compounds according to Robin and Day's classification.

Recently, we[8] and others[9] have extended the area of mixed valence systems to the field of covalently bonded dimetal units by employing two or more dimetal units, typically two Mo_2^{4+} cores joined by an appropriate linker. In such compounds, quadruply bonded Mo_2^{4+} units often act as redox sites. By careful selection of the linker, it is possible to manipulate the molecular structure, regulate the electronic configuration, and tune the chemical properties of the assembled compounds. The compounds that have been most studied may be generically formulated as [Mo_2]L[Mo_2], whereas [Mo_2] is an abbreviation for a Mo_2^{4+} core supported by ligands such as *N, N'*-di(*p*-

anisyl)formamidinate (DAniF) anions, and L is the linker capable of bridging the two [Mo$_2$] units. In addition to organic linkers such as dicarboxylate, $^-$O$_2$C–Y–CO$_2^-$,[10] and diamidate,[11] a variety of inorganic species have been used to link two dimetal units. These include polyatomic anions EO$_4^{2-}$ (E = S, Mo and W),[12] E(OCH$_3$)$_4^{2-}$ (E = Zn or Co),[13] single atom hydride H$^-$,[14] hydroxide OH$^-$,[15] halides X (X = Cl$^-$, Br$^-$ and I$^-$),[15b] and alkoxides $^-$OR (R = CH$_3$, CH$_2$CH$_3$).[16]

To a certain extent, a covalently bonded dimetal unit behaves like a single metal ion. For this reason, the "dimer of dimers" complexes, [M$_2$]L[M$_2$], have a basic kinship with the binuclear Creutz-Taube ion. For instance, the [M$_2$] unit is an electrochemically addressable redox center in which one-electron oxidation from this type of center occurs reversibly, and the "dimer of dimers" displays two successive redox couples with varied potential separations. This separation between two redox waves, usually denoted as $\Delta E_{1/2}$, has been commonly used to estimate the electronic coupling between the two metal centers. Similarly to binuclear complexes with two redox sites, a constant can also be assigned for the comproportionation equilibrium (Eq. 1) involving dimetal species at three different oxidation levels. This comproportionation constant, K_c, is exponentially related to $\Delta E_{1/2}$,[17] and can be calculated using Eq. 2. Because the value of K_c measures the thermodynamic stability of the mixed-valence species, here in the dimetal case the $\{[M_2]L[M_2]\}^+$, it has widely been used to evaluate the strength of electronic communication between the redox sites.

$$[M_2](L)[M_2] + \{[M_2](L)[M_2]\}^{2+} \rightleftharpoons 2\{[M_2](L)[M_2]\}^+ \qquad (1)$$
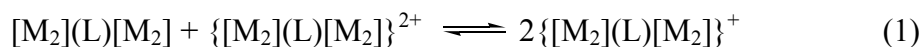
$$K_c = e^{\Delta E_{1/2}/25.69} \qquad (2)$$

Through previous studies of molybdenum dimers of dimers, formulated as [Mo$_2$]L[Mo$_2$], it has been generally established that the efficiency of electronic communication between the [Mo$_2$] units largely (but not solely) depends on the ability of the linker L to conduct electrons from the dimetal centers through itself, or more specifically, the ability of linker to create efficient metal (δ) – ligand (π*) orbital interactions. One good example to this point involves two isomers of [Mo$_2$]L[Mo$_2$] where the linker L is a diaryoxamidate ligand, ¯ArN(O)C–C(O)NAr¯ (Ar = C$_6$H$_5$– or p– CH$_3$OC$_6$H$_4$¯).[11] Denoted as α form and β form (Figure 3), these two isomers are different in the way the linker bridges the two [Mo$_2$] cores. In the α form, the amidate linkers were non planar, with the two ArN(O)C planes being approximately perpendicular. For the β form, the C–C unit and the Mo–Mo bonds are essentially parallel to each other, and the oxidized species have a heteronaphthalene–like structure. Electrochemical studies show that the two isomers have distinct electronic communication as the $\Delta E_{1/2}$ value for the two successive redox waves is significantly larger for the β isomer than the α isomer. One possible explanation for this phenomenon is that in the β form, the Mo$_2$ units and the coordinating nitrogen and oxygen atoms form a perfect plane, which adequately provides a platform for efficient metal (δ) to ligand (π*) orbital overlap. In this way, electrons from the dimetal centers may flow from one end to the other through this conjugated system with significantly lower energy barrier than in the case of α form, where the conformation of the bridging style of the linker makes it impossible to obtain a well conjugated system for the electrons to move through.
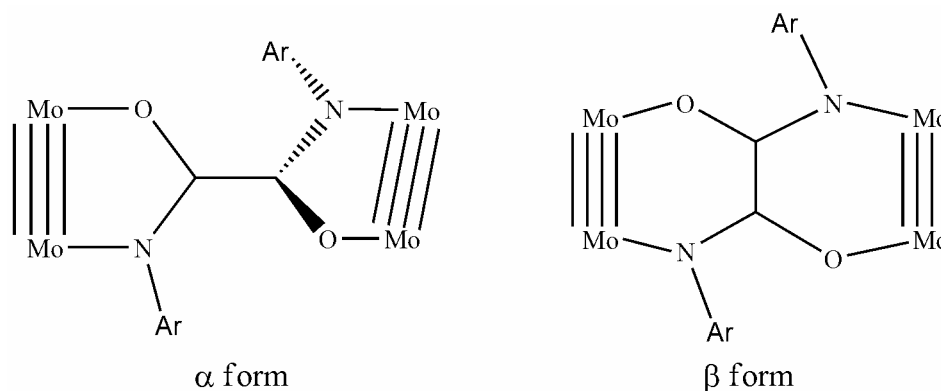
Figure 3. α and β isomer of the $[Mo_2][^-ArN(O)C–C(O)NAr^-][Mo_2]$ complex, where $[Mo_2] = [Mo_2(DAniF)_3]^+$.

The work to be presented here in this thesis mainly focuses on the syntheses of molybdenum dimer of dimers connected by a variety of linkers and the electronic communication between $[Mo_2]$ units in these synthesized compounds. With regard to the type of linkers used, all these compounds are divided into two categories: 1) $[Mo_2]$ dimers bridged by inorganic metal complexes with open coordination sites, to be covered in Chapter II, and 2) $[Mo_2]$ dimers bridged by organic ligands of substituted zwitterionic quinines, to be covered in Chapter III. Common synthetic precursors in this work include $Mo_2(DAniF)_3(O_2CCH_3)$ and $[Mo_2(cis\text{-}DAniF)_2(NCCH_3)_4](BF_4)_2$. Upon treatment of sodium methoxide (methanol solution), the acetate group in $Mo_2(DAniF)_3(O_2CCH_3)$ is replaced by one methoxide anion and one methanol molecule,[18] which facilitates linker ligands such as isonicotinate ions and substituted zwitterionic quinones, to come in and replace the acetate groups. In the precursor $[Mo_2(cis\text{-}DAniF)_2(NCCH_3)_4](BF_4)_2$, since acetonitrile molecules are labile ligands, they can be easily replaced by other desired ligands like the isonicotinate ions.

In chapter II, linkers that are used to connect two different dimolybdenum building blocks include single metal complexes, such as $ZnCl_2$ and $Ni(acac)_2$ (acac = acetyl acetonate), as well as dimetal complex like $Rh_2(O_2CCH_3)_4$. The dimers of dimers synthesized in this part are invariably synthesized through self-assembly of individual neutral molecules, usually with two [Mo_2] moieties on two ends and another complex of a different metal sandwiched in between, therefore, they can be called "molecules of molecules", or supramolecules. These supramolecules are interesting in the structural point of view, in that they bear shapes varying from molecular rods, to distorted squares, to even zigzag shaped infinite chains. The $Mo_2\cdots Mo_2$ separations are exceptionally long in the synthesized supramolecular structures, with the molecular rod $Mo_2(DAniF)_3(O_2CC_5H_4N)-Rh(O_2CCH_3)_4-Mo_2(DAniF)_3(O_2CC_5H_4N)$ having the longest separation (21 Å) observed so far for molybdenum dimers of dimers. Electrochemical studies show only one redox wave for each dimer of dimers in this part, indicating that the electronic communication between Mo_2^{4+} units are very weak, making these systems fall into Class I of the Robin-Day categories. This result is understandable because electronic coupling normally decreases drastically with increasing distance, therefore it is difficult for electrons to flow all the way through the long distances between the molybdenum redox sites in these systems.

Chapter III focuses on a couple of molybdenum dimers of dimers that are different from the ones seen in Chapter II in terms of the type of linkers that are involved. Rather than inorganic complexes, organic ligands of substituted zwitterionic quinones, namely 1,2-dihydroxyl-4,5-dimethylaminbenzene and 1,3-dihydroxyl-2,5-dimethylaminbenzene are used to connect [Mo_2] units. When intramolecular electronic

communication is concerned, the main advantages of using this type of ligands over the previous ones are: 1) the synthesized structure contains a perfectly flat plane defined by the two Mo_2^{4+} cores, the coordinating atoms and the phenyl ring of the bridging ligand, which potentially provides a platform for a well conjugated system, 2) metal to ligand orbital overlap proved to be very efficient, and 3) $Mo_2\cdots Mo_2$ distances are relatively short so that electronic coupling is not hindered. Experimental results demonstrated very strong electronic communication between the dimolybdenum units and exceptionally large $\Delta E_{1/2}$ and K_c values were observed with the larger one being 2.34×10^{14}, the largest observed so far with molybdenum dimer of dimers.

CHAPTER II

A DELIBERATE APPROACH FOR THE SYNTHESES OF HETEROMETALLIC SUPRAMOLECULES CONTAINING DIMOLYBDENUM Mo_2^{4+} SPECIES COORDINATED TO OTHER METAL UNITS*

The use of coordination bonds and weak interactions for the creation of extended arrays containing metal units connected by organic linkers is of great importance.[19] In metal-based supramolecules and nanostructures, the metal units play an important role in extending the dimensions of the molecules, controlling the structural geometries and tuning the chemical and physical properties of the compounds.[20,21] The basic strategy for the formation of discrete molecules or molecular assemblies with desirable size, shape and topology is to manipulate the relationship between the metal unit and organic linker using basic principles of transition metal chemistry[22] with the idea of developing functionalized molecules or molecular aggregates. Indeed, elegant design and synthesis have resulted in metal-ligand hybrid molecules that show potential applications as electronic devices and materials, for example, single molecular transistors[23] and single molecule magnets,[24] which are desirable because of their conducting,[25] magnetic[25c,26] and optical properties.[27]

Contrary to the synthesis of organic compounds with multiple functional groups that can be achieved with high specificity by use of well-defined reactions and reagents, creation of large metal-based molecules with a high degree of complexity remains highly challenging because of the dynamic properties and lability of many coordination bonds. A self-assembly approach could be an efficient way to achieve an ordered structure, but such approach depends largely on the availability of programmed metal-based building blocks but these are generally rare.

In recent years, we have been able to create extended supramolecular architectures through convergent synthesis[28,29] by employing covalently bonded building blocks having dimetal units with a hierarchy of ligand labilities, such as those of the types $[M_2(DAniF)_n(NCCH_3)_{2(4-n)}]^{(4-n)+}$ and $M_2(DAniF)_n(O_2CCH_3)_{4-n}$ (M = Mo,[11a,30] Rh[31] or Ru[32]). In a few of these compounds there are different metal units involved, for example, $[Mo_2(DAniF)_3]_2(OCH_3)_2M(CH_3O)_2[Mo_2(DAniF)_3]$ (M = Zn and Co)[13a] and $[Mo_2(DAniF)_3]_2(O_2MO_2)[Mo_2(DAniF)_3]$ (M = Mo and W).[12]

The latter are examples of rare heterometallic superstructures that may have potential applications as molecular devices[33] in addition to their interest in fundamental chemistry. In this report a deliberate synthesis for compounds having metal–metal bonded units combined with single metal or other dimetal units that help increase structural diversity is presented. In this "ligand-directed" approach, a functionalized ligand is used to generate various metal nuclearities. In the designed corner pieces, $Mo_2(DAniF)_3(O_2CC_5H_4N)$ (**1**) and *cis*-$Mo_2(DAniF)_2(O_2CC_5H_4N)_2$ (**2**), either one or two bifunctional isonicotinate ligands, $[O_2CC_5H_4N]^-$, are incorporated. The carboxylate group binds to the dimolybdenum unit and the tethered pyridyl nitrogen donor atom acts as the

hook in a fishing pole to attract and then bind to other metal centers (**II** in Scheme 1). Thus the isonicotinate group may act as an *adapter* between dimetal units and single metal, or other dimetal species. A reported example that used a similar approach was that

Scheme 1

of the dirhenium building block *cis*-[Re$_2$(dppm)$_2$(O$_2$CC$_5$H$_4$N)$_2$], prepared for the syntheses of heterometallic oligomers.[34]

The building blocks **1** and **2** are programmed to incorporate different metal units through a binary assembly reaction. Because of geometric constraint in each precursor, the resultant aggregates have predictable structural motifs. The heterometallic supramolecules synthesized by self-assembly of **1** with selected metal complexes include two molecular rods, **1**-Ni(acac)$_2$-**1** (**3**) and **1**-Rh$_2$(O$_2$CCH$_3$)$_4$-**1** (**4**). Using the cisoid

compound **2** as starting material, a molecular rhombus, [**2**-Zn(Cl$_2$)]$_2$ (**5**) was made. All these compounds have been structurally characterized using X–ray crystallography.

Results and Discussion

Syntheses of Dimolybdenum Building Blocks. The mixed-ligand, quadruply bonded paddlewheel complexes **1** and **2** were prepared at room temperature by ligand substitution reactions from the precursors Mo$_2$(DAniF)$_3$(O$_2$CCH$_3$)[11a] and [*cis*-Mo$_2$(DAniF)$_2$(NCCH$_3$)$_4$](BF$_4$)$_2$,[30] respectively, according to Eqs. 3 and 4.

$$\text{Mo}_2(\text{DAniF})_3(\text{O}_2\text{CCH}_3) \;+\; \text{HO}_2\text{CC}_5\text{H}_4\text{N} \xrightarrow[\text{rt}]{\text{NaOCH}_3/\text{THF}} \text{Mo}_2(\text{DAniF})_3(\text{O}_2\text{C}_5\text{H}_4\text{N}) \tag{3}$$

$$\textit{cis-}[\text{Mo}_2(\text{DAniF})_2(\text{NCCH}_3)_4]^{2+} \;+\; 2\text{HO}_2\text{CC}_5\text{H}_4\text{N} \xrightarrow[\text{rt}]{\text{NaOCH}_3/\text{NCCH}_3}$$
$$\textit{cis-}\,\text{Mo}_2(\text{DAniF})_2(\text{O}_2\text{C}_5\text{H}_4\text{N})_2 \tag{4}$$
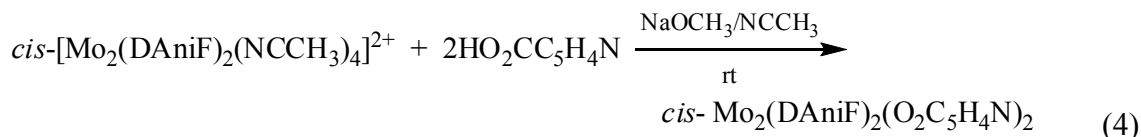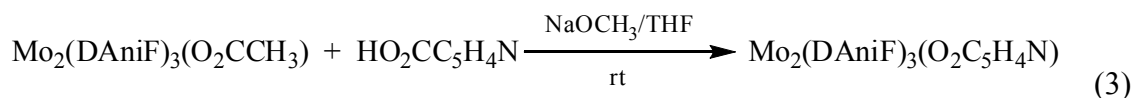
The first equation represents a two step process. In this reaction replacement of the acetate group in Mo$_2$(DAniF)$_3$(O$_2$CCH$_3$) by an isonicotinate ligand is needed. Because both of the leaving and incoming groups are carboxylates, direct ligand exchange is generally inefficient, as shown for example during the conversion of *cis*-ReCl$_2$(μ-dppm)$_2$(O$_2$CCH$_3$)$_2$ into *cis*-ReCl$_2$(μ-dppm)$_2$(O$_2$CC$_5$H$_4$N)$_2$, which required reflux of the reaction mixture over a period of two days.[34] The carboxylate replacement process has now been improved by using NaOCH$_3$ to remove the acetate group in a reaction that forms the intermediate compound Mo$_2$(DAniF)$_3$(OCH$_3$)(CH$_3$OH),[35] which was then treated with neutral isonicotinic acid. This intermediary does not have to be isolated nor

purified, and this two-step, one-pot reaction gives the monodentate building block **1** in good yield.

Substitution of acetonitrile molecules in [*cis*-Mo$_2$(DAniF)$_2$(NCCH$_3$)$_4$]$^{2+}$ by isonicotinate groups for the preparation of **2** is convenient and straightforward because of the high lability of the CH$_3$CN molecules. In principle, this reaction resembles that for the preparation of *cis*-Mo$_2$(DAniF)$_2$(O$_2$CCH$_3$)$_2$, made by mixing the precursor with an excess of sodium acetate.[18] For the synthesis of **2**, the isonicotinate anion was generated *in situ* by addition of sodium methoxide to a mixture of the dimolybdenum precursor and nicotinic acid in acetonitrile. The neutral corner piece **2**, which has a low solubility in polar solvents, readily precipitates from the reaction mixture. Compound **2** appears to be stable and there is no evidence for a *cis* to *trans* isomerization.

The two corner pieces **1** and **2** are isolated in good purity as shown by their ^{1}H NMR spectra in CDCl$_3$. For **1**, there are two singlets at 8.54 and 8.44 ppm in a ratio of 1:2 that correspond to the methine protons from the formamidinate ligands *trans* and *cis* to the isonicotinate group, respectively. The aromatic protons from the isonicotinate ligands are deshielded, and appear at low field as two apparent doublets, one centered at 8.78 ppm and the other one at 8.11 ppm. The aromatic protons from the two types of hydrogen atoms of the anisyl groups appear as two sets of signals, one for the groups *cis* to the isonicotinate group and the other one for the *trans* protons. These appear as pseudo doublets centered 6.51 and 6.28 ppm, and 6.68 and 6.59 ppm, respectively. Finally, the signals for the methoxy groups of the anisyl groups appear as singlets at 3.76 (12 H) and 3.70 (6 H). The UV-vis absorption at 464 nm (2.4 × 10^4 M^{-1}·cm^{-1}) is within the range of the δ→δ* transitions in quadruply bonded compounds of this type.[8] The ^{1}H NMR

spectrum of **2** in CDCl$_3$ suggests the presence of a highly symmetrical species in solution. There are two signals (centered at 8.75 and 8.04 ppm) for the two types of hydrogen atoms in the isonicotinate anion and only one singlet for the methine hydrogen atom at 8.44 ppm. The aromatic groups of the formamidinate groups are also equivalent and the signals centered at 6.63 ppm. A singlet at 3.72 ppm corresponds to the hydrogen atoms in the methoxy groups.

Syntheses of Large Arrays. Because of the dangling pyridyl groups, the dimolybdenum building blocks **1** and **2** may be viewed as monodentate or bidentate ligands, respectively, capable of binding to another metal unit through a coordination bond. In both compounds the linker is preinstalled, e.g., the pyridyl group $-C_5H_4N\rightarrow$ is attached to the Mo$_2^{4+}$ unit and is accessible to bind a Lewis acid. With these preprogrammed building blocks, heterometallic supramolecules can be prepared by efficient and straightforward binary self-assembly reactions. Compound **1** has been used for the preparation of hybrid molecules having three discrete metal centers, and the corner piece **2** in combination with single metal unit ZnCl$_2$ for the preparation of a molecular rhombus.

By mixing **1** and Ni(acac)$_2$ in a 2:1 stoichiometric ratio at ambient temperature compound **3** is prepared in reasonable yield. Likewise reaction of **1** with strong Lewis acids having Rh$_2^{4+}$ paddlewheel cores such as dirhodium tetraacetate leads to the formation of **4**, in which an Rh$_2^{4+}$ unit is located between two dimolybdenum units. Both **3** and **4** are rod-like molecules (*vide infra*).

Because of its ligand arrangement, the corner piece **2** is expected to give molecules having different geometries than those from reactions using **1**. In a reaction

with the tetrahedrally coordinated $ZnCl_2(THF)_2$ species and **2**, the labile THF molecules were easily replaced by the dangling N-donor pyridyl groups to generate a cyclic heterometallic oligomer **5** having the shape of a rhombus.[36]

All the assembled molecules (**3**, **4** and **5**) are neutral. Their solubility is generally low in polar solvents, such as ethanol and acetonitrile, but fairly high in dichloromethane. This difference in solubility in polar and non polar solvents is helpful for product purification and crystal growth, and facilitates product characterization in both solid state and in solution.

Structures. As shown in Figure 4a, compound **1** has a quadruply bonded Mo_2^{4+} unit equatorially coordinated by three formamidinate (DAniF) ligands and one isonicotinate ($O_2CC_5H_4N$) group that is coordinated to the dimetal unit through the carboxylate terminus. This arrangement leaves a dangling pyridyl moiety capable of serving as an angler for the capture of metal-containing Lewis acids. The Mo–Mo bond distance, 2.0906(5) Å, is typical for quadruply bonded dimolybdenum units embraced by four, three-atom bridging ligands, such as $Mo_2(DAniF)_4$[37] and $Mo_2(OCCH_3)_4$.[38] As designed, this molecule is closely related to that of its precursor $Mo_2(DAniF)_3(O_2CCH_3)$ by having the same coordination sphere and a similar Mo–Mo bond length [39] of 2.0892(8) Å. Upon replacement of the acetate by an isonicotinate group, the color of the compounds changes from yellow to red as the $\delta \rightarrow \delta^*$ transition is shifted from 439 nm to 464 nm. In the solid state, the pyridyl group is not in the plane defined by the dimetal unit and the CO_2 bridging group; the torsion angle is about 24°.

In **2** there are two cisoid DAniF and two isonicotinate anions surrounding the Mo_2^{4+} unit, as illustrated in Figure 4b. The Mo–Mo bond length, 2.115(2) Å, is 0.02 Å

longer than that of 2.092(2) Å in *cis*-Mo$_2$(DAniF)$_2$(O$_2$CCH$_3$)$_2$,[8] a molecule with a similar core. Even though this bond length is slightly elongated, the distance falls in the range of dimolybdenum quadruply bonded distances. The two orthogonal pyridyl groups are slightly tilted relative to the five-membered chelating rings $\overbrace{\text{O—Mo—Mo—O—C}}$ and the torsion angles are 5.90° and 14.45°.
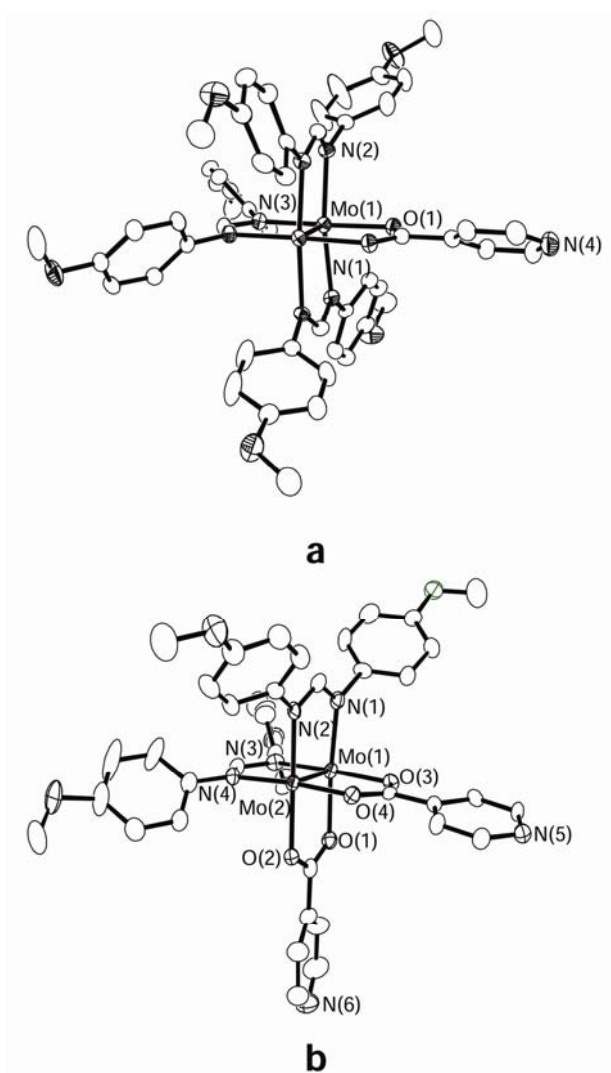
Figure 4. Molecular structures of the building blocks **1** (a) and **2** (b). Displacement ellipsoids are drawn at the 40% probability level. All hydrogen atoms have been omitted for clarity.

The rod-like compound **3** may be described by the formula **1**–Ni(acac)$_2$–**1**. The two Mo$_2^{4+}$ units are connected through isonicotinate termini to a planar Ni(acac)$_2$ unit as shown in Figure 5. This compound crystallized in the space group $P\bar{1}$ with the molecule residing on a general position. Because the isonicotinate linkers are slightly bent the molecule is slightly curved. This hybrid rod is long when compared to other "dimers of dimers" synthesized using the [Mo$_2$(DAniF)$_3$]$^+$ building block. The distance between the two dimetal centers is about 18 Å. The longest Mo$_2\cdots$Mo$_2$ separation, about 16 Å, was reported in a compound having the conjugated dicarboxylate linker, deca-2,4,6,8-*trans*, *trans*, *trans*, *trans*-octatetraene-1,10-dioate.[10b] In **3**, the two crystallographically independent Mo–Mo bonds are chemically equivalent (bond lengths of 2.0927(7) and 2.0923(7) Å) and are essentially parallel to each other. The two pyridyl groups on the apices of the octahedrally coordinated Ni^{2+} moiety are essentially co-planar and mutually define a plane that bisects the NiO$_4$ square. The torsion angles (*ca*. 2°) between each of the pyridyl rings and the corresponding $\overline{\text{O—Mo—Mo—O—C}}$ groups are significantly smaller than in **1** (*ca*. 24°).
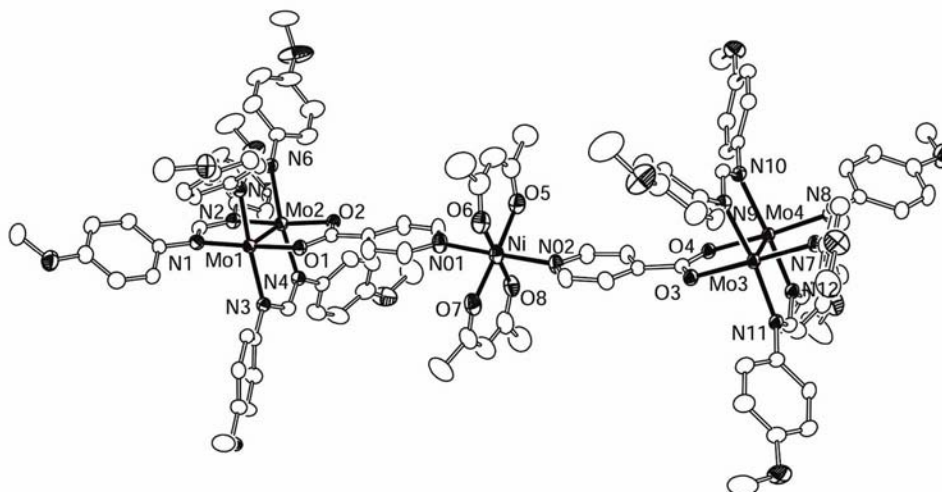
Figure 5. Molecular structure of **3** in **3**·2CH$_2$Cl$_2$ drawn with displacement ellipsoids at the 40% probability level. All hydrogen atoms have been omitted for clarity.

The rod **4**, described by the formula **1**-Rh(O$_2$CCH$_3$)$_4$-**1**, crystallized in the triclinic $P\bar{1}$ space group with $Z = 1$. This molecule has an inversion center at the midpoint of the Rh–Rh bond. As shown in Figure 6, there are two basically parallel Mo$_2^{4+}$ units at the ends of the rod. A central Rh$_2^{4+}$ unit has the dirhodium single bond essentially perpendicular to the dimolybdenum units. The separation between the two Mo$_2^{4+}$ units of about 21 Å is the longest among all dimolybdenum pairs synthesized to date. The crystallographically independent Mo–Mo bond distance, 2.0925(8) Å, is almost identical to those in **1** and **3** (Table I). The Rh–Rh bond length of 2.402(1) Å and the Rh–N distance of 2.240(4) Å are comparable to those in Rh$_2$(O$_2$CCH$_3$)$_4$(py)$_2$.[40] The molecule has a highly symmetrical arrangement having idealized D_{2h} symmetry. The two pyridyl groups have torsion angles of 5.5°, much smaller than that of 24° in the building block **1**.

Table I. Selected Bond Lengths (Å) and Angles (deg) for **1– 5**.

	1	2 ·2CH$_2$Cl$_2$	3 ·2CH$_2$Cl$_2$	4 ·4.5CH$_2$Cl$_2$·C$_6$H$_{14}$	5 ·4CH$_2$Cl$_2$
Mo(1)−Mo(2)		2.115(2)	2.0925(8)	2.0926(8)	2.0920(7)
Mo(1)−Mo(1A)	2.0905(5)				
Mo(3)−Mo(4)			2.0923(7)		
Mo(1)−N(1)	2.147(2)	2.103(11)	2.109(3)	2.142(4)	2.109(4)
Mo(1)−N(3)	2.123(2)	2.110(10)	2.139(3)	2.162(4)	2.104(4)
Mo(1)−N(5)			2.137(3)	2.161(5)	
Mo(2)−N(2)		2.105(10)	2.138(3)	2.133(4)	2.118(3)
Mo(2)−N(4)		2.120(10)	2.136(3)	2.123(4)	2.114(4)
Mo(2)−N(6)			2.169(3)	2.161(4)	
Mo(1)−O(1)	2.145(2)	2.127(9)	2.144(3)	2.137(3)	2.123(3)
Mo(1)−O(3)		2.139(8)			2.149(3)
Mo(2)−O(2)		2.140(8)	2.124(3)	2.148(3)	2.136(3)
Mo(2)−O(4)		2.138(8)			2.111(3)
N(1)−Mo(1)−O(1)	85.73(7)	175.4(4)	174.3(2)	87.9(1)	174.7(1)
N(3)−Mo(1)−O(1)	175.23(6)	88.7(4)	88.0(1)	175.3(1)	85.3(1)
N(5)−Mo(1)−O(1)				84.0(1)	
N(2)−Mo(2)−O(2)		174.1(4)	174.2(1)	88.5(1)	175.6(1)
N(4)−Mo(2)−O(2)		89.4(4)	85.1(1)	174.1(2)	87.3(1)
N(6)−Mo(2)−O(2)			86.4(1)	88.3(2)	
N(1)−Mo(1)−N(3)		94.6(4)	88.6(1)	94.0(2)	95.3(1)
N(1)−Mo(1)−N(5)			95.4(1)	170.3(2)	
N(2)−Mo(2)−N(4)		93.9(4)	90.9(1)	93.6(2)	95.3(1)
N(2)−Mo(2)−N(6)			97.2(1)	174.2(2)	
O(1)−Mo(1)−O(3)		88.5(3)			85.9(1)
O(2)−Mo(2)−O(4)					86.5(1)
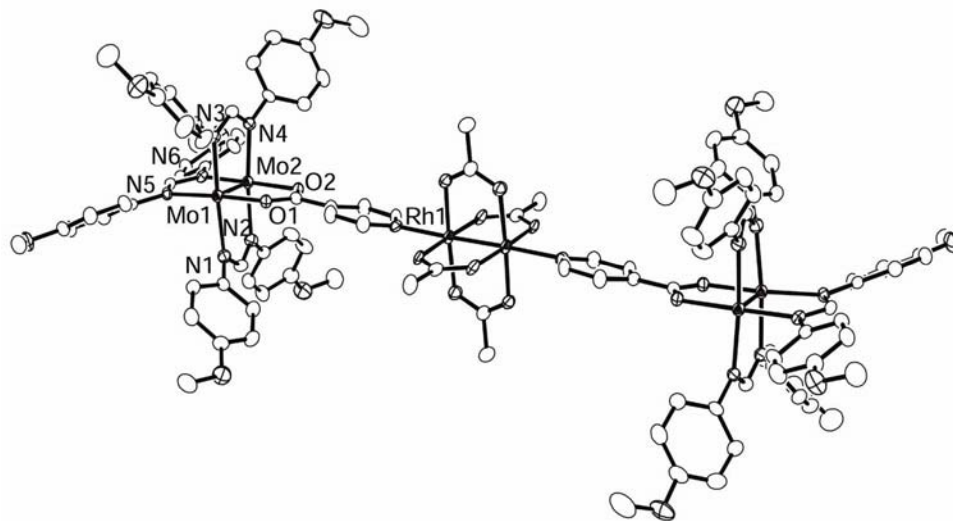
Figure 6. Molecular structure of **4** in **4**·4.5CH$_2$Cl$_2$·C$_6$H$_{14}$ drawn with displacement ellipsoids at the 40% probability level. All hydrogen atoms have been omitted for clarity.

In compound **5**, Zn^{2+} moieties serve as linkers between the cisoid Mo$_2^{4+}$ units. The compound crystallized in the space group $P2_1/n$. In each unit cell, there are two crystallographically independent molecules residing on special positions. This supramolecule is a distorted rhombus with alternating Zn^{2+} and Mo$_2^{4+}$ metal units at the vertices and four isonicotinate groups serving as edges (Figure 7). The formula may be abbreviated as [**2**-ZnCl$_2$]$_2$. The Mo–Mo distances of 2.0920(7) Å are slightly shorter than in the building block **2** but similar to those in **1**, **3** and **4**. The Zn···Zn separation of 11.935 Å, measured from the centers of the two Mo$_2^{4+}$ units, is shorter than the other diagonal length, 13.475 Å. The geometry for the ZnCl$_2$N$_2$ moiety is that of a distorted tetrahedron. The N–Zn–N angle, 102.8°, is slightly smaller than the ideal value of 109.5° while the Cl–Zn–Cl angle, 119.63(8)° is larger. The molecule defines a diamond shaped area with

an approximate dimension of 9 Å × 9 Å and hosts one interstitial dichloromethane molecule disordered over two orientations.
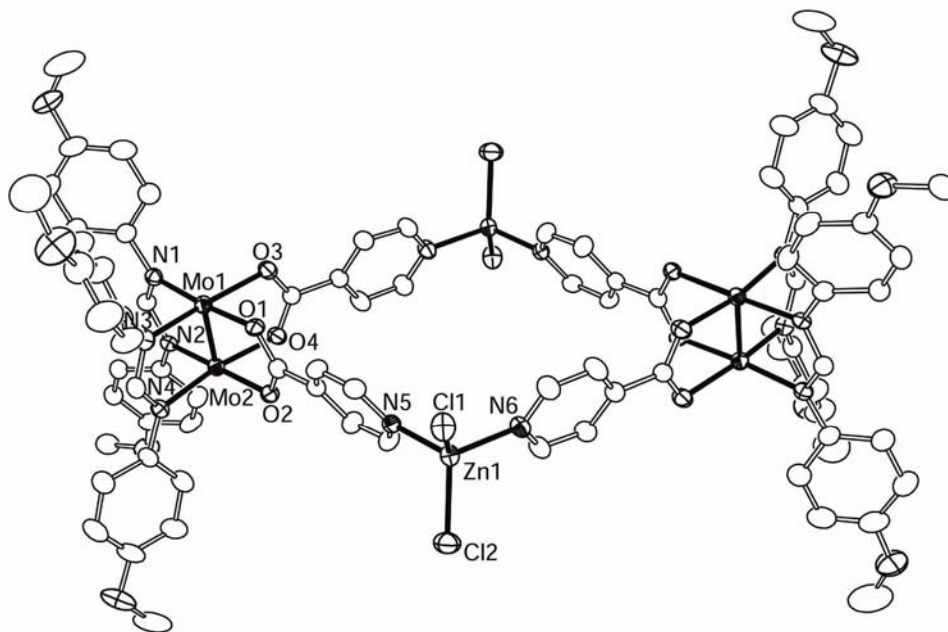
Figure 7. Molecular structure of **5** in **5**·4CH$_2$Cl$_2$ drawn with displacement ellipsoids at the 40% probability level. All hydrogen atoms have been omitted for clarity.

Information on the structures in solution of these large molecules has been obtained by ^{1}H NMR spectroscopy. Compounds **4** and **5** are diamagnetic because of the presence of two quadruply bonded Mo$_2$$^{4+}$ units and the singly bonded Rh$_2$$^{4+}$ unit in **4** and the d^{10} electronic structure of the Zn^{2+} units in **5**. For the rod-like **4**, the spectrum in CDCl$_3$ shows a singlet at 8.59 ppm corresponding to the methine hydrogen atoms from the formamidinate ligands *trans* to the isonicotinate ligands. The signals for the *cis* methine ligands overlap with some of the isonicotinate signals at 8.46 ppm while the other signals for the isonicotinate are centered at 9.48 ppm. The rest of the signals,

including the singlet at 1.96 ppm for the methyl groups from the $Rh_2(O_2CCH_3)_4$ moiety, are in the expected regions of the spectrum for a highly symmetrical species. Therefore the spectrum is consistent with the solid state structure. Similarly for **5**, the simple pattern of the spectrum with only two singlets at 8.47 and 3.72 ppm for the methine and methoxy groups and the expected pattern for the aromatic hydrogen atoms indicate that the shape of the molecule in solution resembles that in the solid state.

Unlike **4** and **5**, compound **3** is paramagnetic with two unpaired electrons per molecule (μ_{eff} = 3.4 BM), as determined from bulk magnetic susceptibility measurements. The source of the paramagnetism is the octahedral coordination of the Ni^{2+} ions derived from the coordination of the two pyridyl groups to the square planar $Ni(acac)_2$ moiety. Species with octahedral *trans*-$Ni(O)_4(N)_2$ units are typically paramagnetic as in *trans*-$Ni(acac)_2(amine)_2$ compounds for which the μ_{eff} have been reported to be in the range of 3.2–3.4 BM.[41] Despite the paramagnetism of **3**, its ^1H NMR spectrum in CD_3Cl shows mostly sharp signals in the expected regions of the spectra. For example, there are singlets with a ratio of 2:1 at 8.31 and 8.45 ppm for the methine and 3.71 and 3.64 ppm for methoxy protons, respectively, from the DAniF ligands. The signals for the anisyl groups are also as expected (6.17–6.60 ppm). However, close inspection of the spectrum shows that the signals from the ligands directly bound to the Ni^{2+} unit are absent. Even when the spectral window was opened to cover the region between −150 ppm and +150 ppm, signals from the acac methyl groups and from the isonicotinate groups were absent. The sharpness of the signals from the anisyl groups and the absence of those in the Ni^{2+} units suggest that there is little or no electronic communication through the isonicotinate bridge, consistent with the electrochemical data below.

Electrochemistry. Cyclic voltammograms (CVs) and differential pulse voltammograms (DPVs) for **1–5** were measured in CH_2Cl_2 solutions. The corner pieces **1** and **2** show reversible one-electron redox processes at 310 and 560 mV vs. Ag/AgCl, respectively (Figure 8). Previous studies on *dimer of dimers* have shown that the separation between the two Mo_2 units is a very important factor in determining whether electronic communication is efficient or not.[8] As the intermetal separations increase, it has often been observed that electronic communication decrease according to an exponential law.[42] Because the separations between the Mo_2 units in **3** and **4** are the longest known for any *dimer of dimers* compounds of this type, an extremely weak communication may be anticipated. This is consistent with the electrochemical data (see Figure 8). Compounds **3** and **4** show very similar patterns in the CVs and DPVs, a redox wave was observed for each one of them between 300 and 400 mV. By analogy to the *dimer of dimers* linked by long unsaturated dicarboxylate ligands,[10c] this wave can be assigned to the two unresolved one-electron oxidation processes on each of the dimolybdenum units. The CV for the rhombohedral compound **5** appears to correspond to a less reversible process. It is possible that because of a relatively weak N to Zn interaction, the molecule may decompose upon oxidation.
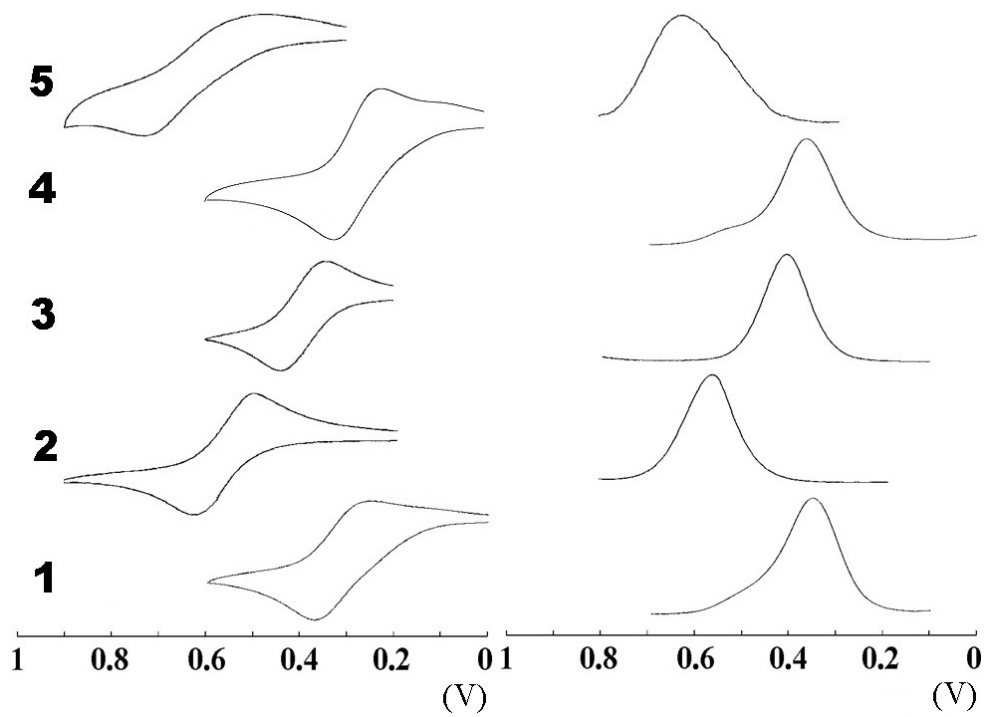
Figure 8. CVs and DPVs (potentials vs Ag/AgCl, in CH₂Cl₂) for compounds **1–5**.

Conclusions. Two new dimolybdenum–containing building blocks Mo$_2$(DAniF)$_3$(O$_2$C$_5$H$_4$N) (**1**) and *cis*-Mo$_2$(DAniF)$_2$(O$_2$CH$_4$N)$_2$ (**2**), each having an angler composed of a pyridyl group capable of binding to metal-containing Lewis acids, have been synthesized. The functionalization by introduction of a bi-functional isonicotinate ligand allows incorporation into **1** and **2** of other metal centers via coordination bonds and the formation of heterometallic supramolecules. By taking advantage of these two programmed building blocks, spontaneous self-assemblies with selective metal complexes, e.g., Ni(acac)$_2$, Rh$_2$(O$_2$CCH$_3$)$_4$ and Zn$_2$Cl$_2$, formation of two metal-based molecular rods **1**-Ni(acac)$_2$-**1** (**3**), **1**-Rh$_2$(O$_2$CCH$_3$)$_4$-**1** (**4**), and a cyclic oligomer [**2**-Zn$_2$Cl$_2$]$_2$ (**5**) have been synthesized. Compounds **3** and **4** are longer than any previously reported dimolybdenum pair. Meanwhile the rhombohedral molecule **5** has a large cavity which holds a CH$_2$Cl$_2$ guest molecule. Incorporation of different metal units into structurally defined architectures is a way to modify the molecular architecture and tune chemical and physical properties. The preparative concept and methodology developed here should have general application for the synthesis of heteronuclear species having metal–metal corner pieces bound to metal-containing Lewis acids.

Experimental Section

Materials and Methods. All manipulations and procedures were performed under a nitrogen atmosphere, using either a nitrogen drybox or standard Schlenk line techniques. Solvents were purified under argon using a Glass Contour solvent purification system or distilled over appropriate drying agents under nitrogen. The starting materials Mo$_2$(DAniF)$_3$(O$_2$CCH$_3$)[11a] and [*cis*-Mo$_2$(DAniF)$_2$(NCCH$_3$)$_4$](BF$_4$)$_2$[30]

were prepared following reported procedures. The dirhodium compound $Rh_2(O_2CCH_3)_4(NCCH_3)_2$ was prepared by treating $Rh_2(O_2CCH_3)_4$[43] with acetonitrile. Commercially available chemicals were used as received.

Physical Measurements. Elemental analyses were performed by Robertson Microlit Laboratories, Madison, New Jersey. Electronic spectra were measured in CH_2Cl_2 solution at ambient temperature on a Shimadzu UV-2501PC spectrometer. ^{1}H NMR spectra were recorded on an Inova-300 or Mercury NMR spectrometer with chemical shifts (δ, ppm) referenced to $CDCl_3$. Cyclic voltammograms and differential pulse voltammograms were collected on a CH Instruments electrochemical analyzer with Pt working and auxiliary electrodes, Ag/AgCl reference electrode, scan rate (for CV) of 100 mV/s, and 0.10 M Bu_4NPF_6 (in CH_2Cl_2) as electrolyte.

Preparation of $Mo_2(DAniF)_3(O_2CC_5H_4N)$, 1. To a yellow solution of $Mo_2(DAniF)_3(O_2CCH_3)$ (0.512 g, 0.500 mmol) in 15 mL of THF, was added 1.0 mL of a $NaOCH_3$ solution (0.5 M in methanol). After stirring for about 2 h, a colorless microcrystalline material, presumably sodium acetate, was removed by filtration. To the filtrate was added an excess of isonicotinic acid (0.080 g, 0.650 mmol). Upon stirring, the color of the mixture immediately changed from yellow to red. After stirring at room temperature for an additional half hour, the solvent was removed under vacuum, and the residue was washed with ethanol (2 × 15 mL), and then dried under vacuum. The red solid was dissolved in dichloromethane (15 mL) and the solution was layered with hexanes. Red block-shaped crystals formed after one day. Yield: 0.380 g (70%). ^{1}H NMR (CDCl$_3$, ppm): 8.78 (d, 2H, isonicotinate), 8.54 (s, 1H, −NC*H*N−), 8.44 (s, 2H, −NC*H*N−), 8.11 (d, 2H, isonicotinate), 6.68 (d, 8H, aromatic), 6.59 (d, 8H, aromatic),

6.51 (d, 4H, aromatic), 6.28 (d, 4H, aromatic), 3.76 (s, 12H, $-OCH_3$), 3.70 (s, 6H, $-OCH_3$). UV-vis, λ_{max} (ε, $M^{-1} \cdot cm^{-1}$): 464 nm (2.4×10^4). Anal. Calcd. for $C_{51}H_{49}Mo_2N_7O_8$: C, 56.72; H, 4.57; N, 9.08. Found: C, 56.49; H, 4.86; N, 9.29.

Preparation of *cis*-Mo₂(DAniF)₂(O₂CC₅H₄N)₂, 2. A mixture of [*cis*-Mo₂(DAniF)₂(NCCH₃)₄](BF₄)₂ (0.520 g, 0.500 mmol) and isonicotinic acid (0.170 mg, 1.38 mmol) was placed in a Schlenk flask. With stirring acetonitrile (*ca*. 20 mL) was added to the solid, producing a blue solution. After about 10 min, 2.0 mL of a sodium methoxide solution (0.5 M in methanol) was added. The color changed from blue to red. The reaction mixture was allowed to stir at room temperature for 3 h. During this period a dark red precipitate formed. The supernatant solution was then decanted. The red solid was washed with 20 mL of ethanol and then dried under vacuum. The crude product was dissolved in dichloromethane (15 mL) and the solution was layered with hexanes. Red needle-shaped crystals formed after 2 days. Yield: 0.24 g (56%). ^{1}H NMR (CDCl₃, ppm): 8.75 (d, 4H, isonicotinate), 8.44 (s, 2H, $-NCHN-$), 8.04 (d, 4H, isonicotinate), 6.63 (m, 16H, aromatic), 3.72 (s, 12H, $-OCH_3$). UV-vis, λ_{max} (ε, $M^{-1} \cdot cm^{-1}$): 450 nm (1.2×10^4). Anal. Calcd. for $C_{42.3}H_{38.6}Cl_{0.6}Mo_2N_6O_8$(**2**·0.3CH₂Cl₂): C, 52.26; H, 4.04; N, 8.64. Found: C, 52.23; H, 3.66; N, 8.78.

Preparation of [Mo₂(DAniF)₃(O₂CC₅H₄N)]₂Ni(C₅H₇O₂)₂, 3. The dimolybdenum building block Mo₂(DAniF)₃(O₂CC₅H₄N) (**1**) (0.400 g, 0.400 mmol) was dissolved in 20 mL of THF. The resulting brownish red solution was transferred into a flask containing Ni(acac)₂ (0.050 g, 0.20 mmol), generating a bright red solution. After the reaction mixture was stirred for an additional 2 h, the solvent was removed under reduced pressure. The red residue was washed with ethanol (*ca*. 15 mL) followed by

hexanes (*ca.*10 mL). The dry solid was dissolved in about 15 mL of dichloromethane and the solution was layered with 40 mL of hexanes, affording red block-shaped crystals after a few days. Yield: 0.285 g (24%). ^{1}H NMR (CDCl$_3$, ppm): 8.54 (s, 2H, −NC*H*N−), 8.31 (s, 4H, −NC*H*N−), 6.60 (d, 16H, aromatic), 6.41 (d, 24H, aromatic), 6.17 (d, 8H, aromatic), 3.71 (s, 24H, −OC*H*$_3$), 3.64 (s, 12H, −OC*H*$_3$). UV-vis, λ_{max} (ε, M^{-1}·mol^{-1}): 474 nm (2.5 × 10^4). μ_{eff} = 3.4 BM. Anal. Calcd. for C$_{115}$H$_{118}$Cl$_6$Mo$_4$N$_{14}$O$_{20}$Ni (**3**·3CH$_2$Cl$_2$): C, 51.70; H, 4.45; N, 7.34. Found: C, 51.33; H, 4.62; N, 7.40.

Preparation of [Mo$_2$(DAniF)$_3$(O$_2$CC$_5$H$_4$N)]$_2$[Rh$_2$(O$_2$CCH$_3$)$_4$], 4. A solution of purple Rh$_2$(O$_2$CCH$_3$)$_4$(NCCH$_3$)$_2$ (0.052 g, 0.100 mmol) and red **1** (0.216 g, 0.200 mmol) was prepared in 20 mL of acetonitrile. The reaction mixture was allowed to stir at room temperature for 4 h. A dark red precipitate formed. The solvent was then removed under reduced pressure. The dark red residue was washed with ethanol (2 × 15 mL). The crude product was dissolved in 15 mL of dichloromethane and the solution was layered with 40 mL of hexanes, affording dark red crystals after one day. Yield: 0.08 g (31%). ^{1}H NMR (CDCl$_3$, ppm): 9.48 (s, 4H, isonicotinate), 8.59 (s, 2H, −NC*H*N−), 8.46 (s, 8H, −NC*H*N− and isonicotinate) 6.72 (d, 16H, aromatic), 6.62 (d, 16H, aromatic), 6.54 (d, 8H, aromatic), 6.33 (d, 8H, aromatic), 3.78 (s, 24H, −OC*H*$_3$), 3.73 (s, 12H, −OC*H*$_3$), 1.96 (s, 12H, −C*H*$_3$). UV-vis, λ_{max} (ε, M^{-1}·cm^{-1}): 499 nm (4.1 × 10^4). Anal. Calcd. for C$_{110}$H$_{110}$Mo$_4$N$_{14}$O$_{24}$Rh$_2$: C, 50.78; H, 4.26; N, 7.53. Found: C, 50.51; H, 4.10; N, 7.72.

Preparation of [*cis*-Mo$_2$(DAniF)$_2$(O$_2$CC$_5$H$_4$N)$_2$][ZnCl$_2$]$_2$, 5. The dimolybdenum building block *cis*-Mo$_2$(DAniF)$_2$(O$_2$CC$_5$H$_4$N)$_2$ (**2**) (0.095 g, 0.100 mmol) was mixed with anhydrous ZnCl$_2$ (0.050 g, 0.37 mmol) in 20 mL of THF. The reaction mixture was stirred for 2 h, during which time a red-purple precipitate formed. The supernatant

solution was decanted and the residue was dried under vacuum. The solid was then extracted with *ca*. 15 mL of dichloromethane and the mixture filtered through a Celite-packed frit. The filtrate was layered with 30 mL of hexanes. Dark red needle-shaped crystals formed after 4 days. Yield: 0.050 g (25%). ^{1}H NMR (CDCl$_3$, ppm): 8.96 (s, 8H, isonicotinate), 8.47 (s, 4H, −NC*H*N−), 8.16 (s, 8H, isonicotinate), 6.60 (m, 32H, aromatic), 3.72 (s, 24H, −OC*H*$_3$). UV-vis, λ_{max} (ε, M^{-1}·cm^{-1}): 508 nm (4.3 × 10^4). Anal. Calcd. for C$_{86}$H$_{80}$Cl$_8$Mo$_4$N$_{12}$O$_{16}$Zn$_2$: C, 44.27; H, 3.45; N, 7.19. Found: C, 44.27; H, 3.52; N, 7.08.

X-ray Structure Determinations. Each crystal was mounted on a cryoloop and centered in the goniometer of a Bruker SMART 1000 CCD area detector diffractometer and then cooled to −60 °C. Cell parameters were determined using the program SMART.[44] Data reduction and integration were performed with the software package SAINT,[45] and absorption corrections were applied using the program SADABS.[46] In all structures, the positions of the heavy atoms were found via direct methods using the program SHELXTL.[47] Subsequent cycles of least-square refinement followed by difference Fourier syntheses revealed the positions of the remaining non-hydrogen atoms. Hydrogen atoms were added in idealized positions. Non-hydrogen atoms were refined with anisotropic displacement parameters. Some of the anisyl group in the DAniF ligands and interstitial CH$_2$Cl$_2$ molecules were found disordered, and they were refined with soft constraints. Crystallographic data for **1**, **2**·2CH$_2$Cl$_2$, **3**·2CH$_2$Cl$_2$, **4**·4.5CH$_2$Cl$_2$·C$_6$H$_{14}$ and **5**·4CH$_2$Cl$_2$ are in Table II, and selected bond distances and angles in Table I.

Table II. X-ray Crystallographic Data for **1**– **5**.

compound	**1**	**2**·2CH$_2$Cl$_2$	**3**·2CH$_2$Cl$_2$	**4**·4.5CH$_2$Cl$_2$·C$_6$H$_{14}$	**5**·4CH$_2$Cl$_2$
empirical formula	C$_{51}$H$_{49}$Mo$_2$N$_7$O$_8$	C$_{44}$H$_{42}$Cl$_4$Mo$_2$N$_6$O$_8$	C$_{114}$H$_{116}$Cl$_4$Mo$_4$N$_{14}$O$_{20}$Ni	C$_{120.5}$H$_{130}$Cl$_9$Mo$_4$N$_{14}$O$_{24}$Rh$_2$	C$_{88}$H$_{84}$Cl$_{12}$Mo$_4$N$_{12}$O$_{16}$Zn$_2$
fw	1079.85	1116.52	2586.47	3067.02	2505.57
space group	*C2/c* (No. 15)	*Pbca* (No. 61)	*P$\bar{1}$* (No. 2)	*P$\bar{1}$* (No. 2)	*P2$_1$/n* (No. 14)
a (Å)	17.615(3)	13.942(7)	14.966(5)	15.260(4)	10.588(3)
b (Å)	18.492(3)	19.41(1)	17.526(6)	16.014(5)	20.103(6)
c (Å)	16.855(3)	35.95(2)	23.141(9)	16.228(5)	24.879(8)
α (deg)	90	90	102.989(7)	108.216(5)	90
β (deg)	118.286(4)	90	98.259(7)	102.413(5)	94.073(5)
γ (deg)	90	90	90.533(7)	106.435(5)	90
V (Å^3)	4835(2)	9726(8)	5848(4)	3406.8(17)	5282(3)
Z	4	8	2	1	2
T (K)	213	213	213	213	213
d$_{calcd}$ (g/cm^3)	1.484	1.525	1.469	1.495	1.575
μ (mm^{-1})	0.580	0.791	0.738	0.840	1.275
R1^a (wR2^b)	0.0453 (0.0798)	0.1264 (0.1816)	0.0817 (0.1380)	0.0847 (0.1588)	0.0625 (0.1194)

^{a} R1 = Σ‖F_o|–|F_c‖/Σ|F_o|.

^{b} wR2 = [Σ[$w(F_o^2–F_c^2)^2$]/Σ[$w(F_o^2)^2$]]$^{1/2}$

CHAPTER III

STRONG ELECTRONIC COUPLING BETWEEN [MO$_2$] UNITS

LINKED BY SUBSTITUTED ZWITTERIONIC QUINONES

The study of electronic interactions between redox centers having structurally identical single metal sites mediated by various bridging groups has been a topic of great interest since the synthesis of the Creutz-Taube ion in the 1960s.[48] Conjugated electron carriers, such as polyenes, polypyrroles and polycondensed aromatics have been utilized as linkers to promote long-range electronic coupling.[49] These complexes not only provide an elegant model for the electron transfer processes in biochemistry, but also have potential for use as molecular wires and single–molecule transistors in a new generation of computers.[50]

Recently our laboratory and others have been interested in analogues containing two dimetal species, usually Mo_2^{4+} units, linked by a variety of bridging ligands,[8,9] in which electronic communication between dimetal units can be conveniently evaluated. Because structural and spectroscopic properties of dimetal units are generally well understood such units provide several advantages for probing electronic coupling.[17] Electrochemistry has been extensively used to probe the degree in which linkers facilitate electronic communication between metal centers by using the well-known relationship that relates comproportionation constants with $\Delta E_{1/2}$ values, $K_c = e^{\Delta E_{1/2}/25.69}$.[8] By carefully selecting and altering the linkers, K_c's ranging from the statistical values of 4 to 6.2 × 10^{13} have been observed.[10b] The most frequently type of ligands used has been dianions of dicarboxylic acids (**V** in Scheme 2) but these lead to low K_c values.[51]

Scheme 2
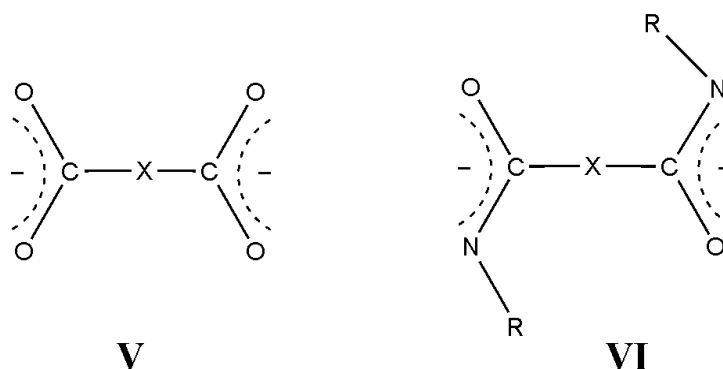
Previous work has shown that amidate ligands (**VI**) possess attractive properties since such groups are much stronger Lewis bases than the carboxylate groups and substituents on the N atoms can be synthetically adjusted both sterically and electronically.[52] Electronic coupling in these amidate bridged compounds is usually much stronger than in those linked by the corresponding carboxylates.

Other ligands that allow strong electronic communication between Mo_2 units are the anion dioxolene (Scheme 3, **VII**) and those of 2,5-dihydroxy-1,4-benzoquinone (dhbq) and its derivatives (**VIII**) ($K_C = 7.9 \times 10^{12}$).[52] Here we report that analogues of the [Mo_2]dioxolane[Mo_2] compound ([Mo_2] represents an Mo_2(formamidinate)$_3$ unit) having two O atoms in the dioxolane linker replaced by isoelectronic N–CH$_3$ groups can be made and one of these compounds give the largest K_c yet known for species containing quadruply bonded Mo_2^{4+} units. These N-substituted benzoquinonemonoimines first made by Braunstein et al.[53] have attracted much attention because they are antiaromatic having $6\pi + 6\pi$ electrons (Scheme 3) Because of the rigidity of the six-membered ring, two

isomers have been isolated, 1,5-dihydroxyl-2,4-dimethylaminbenzene (**IX**, *cis*) and 1,4-dihydroxyl-2,5-dimethylaminebenzene (**X**, *trans*).

Scheme 3

$$\textbf{VII} \qquad \textbf{VIII}$$

$$\textbf{IX} \qquad \textbf{X}$$
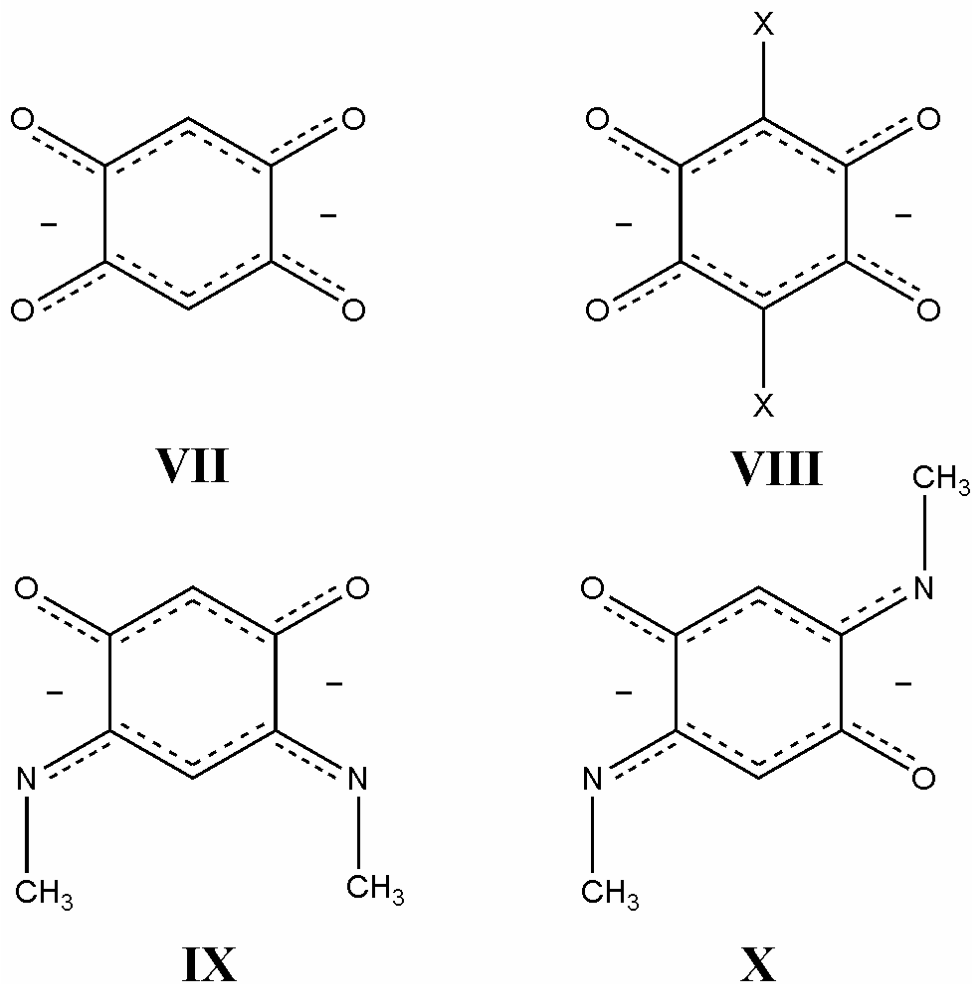
Results and Discussion

Synthesis. The respective *pairs of pairs* having Mo_2 units, isomers **6** and **7**, were synthesized as shown in Eq. 5 by substitution of the labile acetate ligand in $Mo_2(DAniF)_3(O_2CCH_3)$[11a] by the more basic N-substituted benzoquinonemonoimines linkers. Here DAniF represents the anion *N,N'*-di-*p*-anisylformamidinate.

$$2\ Mo_2(DAniF)_3(O_2CCH_3)\ +\ H_2C_8H_8N_2O_2$$

$$\xrightarrow[\text{r.t.}]{2\ NaOCH_3/THF}\ [Mo_2(DAniF)_3]_2(C_8H_8N_2O_2) \tag{5}$$
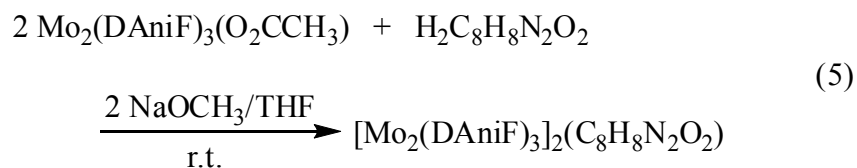
After routine treatment of the respective reaction mixtures, crystals of **6** were obtained by diffusion of ethanol into the solution of **6** dissolved in THF, and crystals of **7** were obtained by diffusion of hexanes into the solution of **7** dissolved in mixed solvents of CH_2Cl_2/acetone (1:1).

Structures. The core structures are shown in Figure 9. Compound **6** crystallized in the monoclinic space group $P2_1/c$ along with five interstitial C_4H_4O molecules in each cell. The linker and the two dimolybdenum units are essentially planar with the two Mo_2 axes essentially paralell to each other. The Mo–Mo distances are 2.0965(10) and 2.0947(10) Å (Table III) and the separation between Mo_2 units is 8.816 Å. Compound **7** crystallized in the triclinic space group P$\bar{1}$ but with $Z = 1$. There are also four interstitial CH_2Cl_2 molecules per cell. The two Mo_2 units are related by an inversion center located at the center of the linker C_6 ring. The two sets of quadruply bonded Mo_2 bonds and the linker are essentially flat, providing what appears to be a well conjugated platform for electron transport between the metal redox sites. This is different from the one linked by dhbq^{2-}, which forms a chair conformation.[52(b)] The Mo–Mo distance of 2.0902(9) Å is within the typical range for Mo–Mo quadruple bonds. The separation between the two Mo_2 units of 8.832 Å is similar to that in **6** and is about 0.3 Å longer than that of the dhbq^{2-} analogue (see Table IV). Importantly both **6** and **7** have significant variations in the C–C bond lengths within the linker C_6 ring, i.e., C(1)–C(2) is 1.470(8) Å and C(2)–

C(3) is 1.386(8) Å for **7**. More detailed C–C bond lengths are listed in Table III. These large differences in C–C bond distances show that the electron conjugation within the ring follows a different pattern than in a typical phenyl ring.
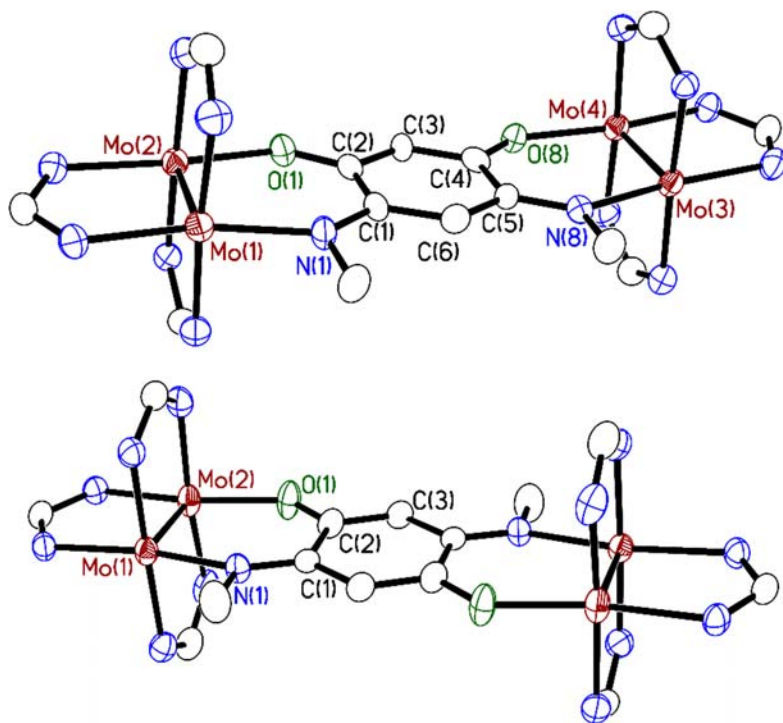
Figure 9. The cores for compounds **6** (up) and **7** (down). Thermal ellipsoids are drawn at the 40% probability level, and all *p*-anisyl groups and hydrogen atoms are omitted for clarity.

Table III. Selected Bond Distances (Å) and Angles (°) for **6** and **7**.

	1	2
Mo(1)–Mo(2)	2.0965(10)	2.0902(9)
Mo(3)–Mo(4)	2.0947(10)	
Mo$_2$···Mo$_2$ ^{a}	8.816	8.832
Mo(1)–N(1)	2.109(7)	2.108(4)
Mo(2)–O(1)	2.076(5)	2.070(4)
Mo(3)–N(8)	2.125(7)	
Mo(4)–O(8)	2.052(5)	
C(1)–C(2)	1.462(11)	1.470(8)
C(2)–C(3)	1.385(11)	1.386(8)
C(3)–C(4)	1.398(11)	
C(4)–C(5)	1.462(11)	
C(5)–C(6)	1.403(11)	
C(6)–C(1)	1.405(11)	
Mo(1)-Mo(2)-O(1)	98.49(16)	99.83(11)
Mo(2)-Mo(1)-N(1)	101.7(2)	100.24(12)
Mo(3)-Mo(4)-O(8)	100.80(15)	
Mo(4)-Mo(3)-N(8)	99.17(18)	

^{a} distances between the midpoints of the [Mo$_2$] units.

Electrochemistry. The cyclic voltammogram (CV) of **6** in CH_2Cl_2 shows two well-separated, reversible waves at 310 mV and 1160 mV (vs Ag/AgCl) (Figure 10). These two redox waves correspond to two one-electron oxidation processes that take place at the [Mo_2] centers. The $\Delta E_{1/2}$ of 850 mV for **6**, represents the largest separation between the two waves in compounds having two quadruply bonded dimolybdenum units joined by any of a large variety of linkers. The corresponding comproportionation constant for **6** is 2.34 $\times$ 10^{14}. For **2** the two $E_{1/2}$ values are 345 mV and 1125 mV. The slightly smaller $\Delta E_{1/2}$ of 780 mV corresponds to a K_c of 1.54 $\times$ 10^{13}.

For comparison, electrochemical data for **6**, **7** and selected [$Mo_2(DAniF)_3$](L)[$Mo_2(DAniF)_3$] compounds are shown in Table IV. These data clearly shows that the family of compounds having benzoquinones and benzoquinonemonoimines show an exceptionally large ability to delocalize electrons with the cis-substituted N-methyl benzoquinonemonoimine being the best. It should be noted that the oxalate linker, which represents the best dicarboxylate linker for electron delocalization has a K_c many orders of magnitude smaller than **6**. Because C–C distances in the six-membered ring of the linker differ significantly for both isomers **6** and **7** (vide supra), electron delocalization is expected to extend through a 14-atom ring that includes the linker and the four Mo atoms (Scheme 2), similarly to the $dhbq^{2-}$ analogue.[52(b)]

Table IV. Electrochemical Data for **6**, **7** and Selected [Mo$_2$(DAniF)$_3$](L)[Mo$_2$(DAniF)$_3$] Compounds.[a]

L	M$_2$···M$_2$ (Å)	$E_{1/2}^{1\,b}$	$E_{1/2}^{2\,b}$	$\Delta E_{1/2}$	K_C	ref
6	8.816	310	1160	850	2.34×10^{14}	This work
7	8.832	345	1125	780	1.54×10^{13}	This work
dhbq^{2-}	8.536	−200	563	763	7.92×10^{12}	51b
ca^{2-}	8.718	−15	780	795	2.75×10^{13}	51b
na^{2-}	---	45	861	816	6.23×10^{13}	51b
oxalate	6.953	294	506	212	3.8×10^{3}	10

[a] Potentials are mV referenced to Ag/AgCl.

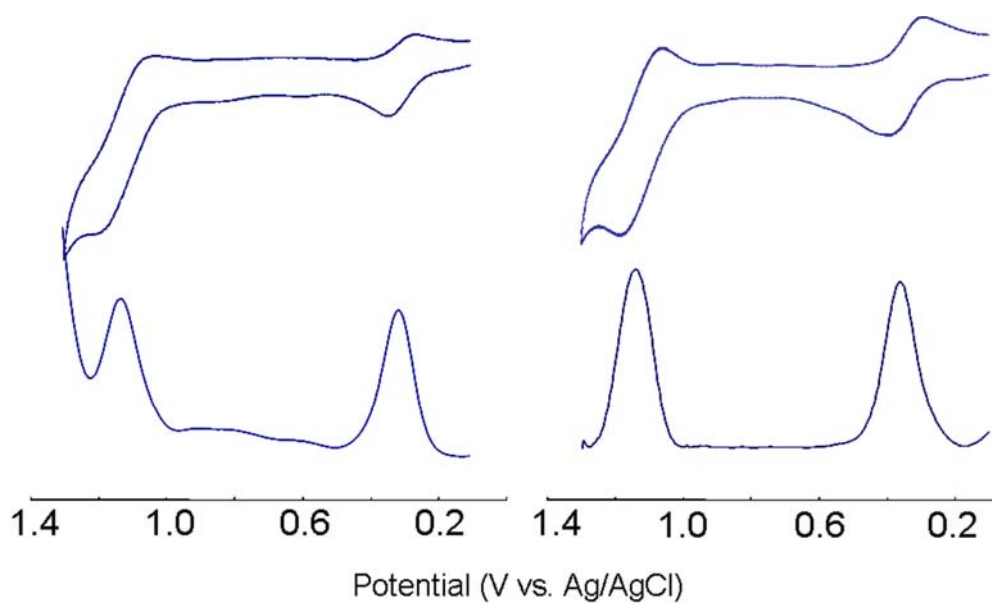[b] $E_{1/2} = (E_{pa} + E_{pc})/2$ obtained from the CV for **6** and **7**.

Figure 10. CVs and DPVs for **6** (left) and **7** (right) recorded in CH$_2$Cl$_2$ solution with potentials referenced to Ag/AgCl.
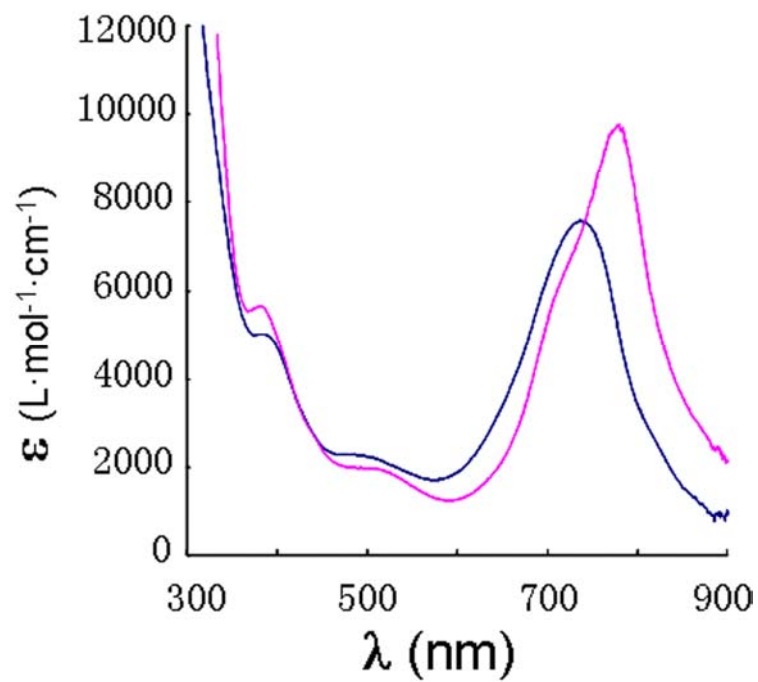
Figure 11. UV-vis spectra for compounds **6** (blue) and **7** (red) in CH$_2$Cl$_2$ solution.

It should also be noted that the electronic spectra for **6** and **7** (Figure 11) show intense absorption bands at 750 nm and 779 nm, respectively. Because the existence of low energy metal-to-ligand charge transfer (MLCT) is critical for the electronic coupling between the dimetal units facilitating an 'electron hopping' pathway,[54] these MLCT bands account not only for the green color of the compounds but are also consistent with the exceptional strong electronic coupling in these species.

Conclusion. The two isomers having [Mo_2] units linked by N–CH_3 substituted benzoquinonemonoimines give *pairs of pairs* with an exceptionally large electronic coupling.

Experimental Section

Material and Methods. All reactions and manipulations were performed under a nitrogen atmosphere, using either a drybox or standard Schlenk line techniques. Solvents were purified under argon using a Glass Contour solvent purification system or distilled over the corresponding drying agent under nitrogen. The starting materials, $Mo_2(DAniF)_3(O_2CCH_3)$[11a] and the linker precursors 1,5-dihydroxyl-2,4-dimethylaminbenzene (**IX**) and 1,4-dihydroxyl-2,5-dimethylaminbenzene (**X**) were prepared according to reported procedures.

Preparation of 1,5-dihydroxyl-2,4-dimethylaminbenzene. [55] Diaminoresorcinol dihydrochloride (0.500 g, 2.35 mmol) was dissolved in 5 ml water and then excess of methylamine solution in water was added. The color changed to purple immediately. This reaction mixture was stirred at room temperature for 30 min and purple crystals appear within 2h. This product was isolated by filtration and washed with cold water.

^{1}HNMR in DMSO (ppm): 3.01 (s, 6H, CH$_3$), 4.95 (s, 1H, aromatic), 5.34 (s, 1H, aromatic), 9.10 (s, 2H, -NH).

Preparation of 1,4-dihydroxyl-2,5-dimethylaminbenzene. [56] Hydroquinone (2.50 g, 0.0227 mol) was placed in a 250ml beaker, to which 30 mL of CH$_3$NH$_2$ aqueous solution (40 wt.%) was then added. The reaction solution first appeared a clear yellow color, and then slowly turned to dark red. After about 30 minutes, dark red crystals were observed at the bottom of the beaker. After 6 hours the crystals were collected through filtration and washed with ca. 10 mL portion each of water, ethanol, and diethyl ether. ^{1}HNMR in CDCl$_3$ (ppm): 2.89 (d, 6H, −CH$_3$), 5.28 (s, 2H, aromatic), 6.59 (s, broad, 2H, −NH).

Preparation of [Mo$_2$(DAniF)$_3$]$_2$\{*cis*-C$_6$H$_2$(ONCH$_3$)$_2$\}, 6. A suspension of 1,5-dihydroxyl-2,4-dimethylaminbenzene (33 mg, 0.20 mmol) in 15 mL of THF was cooled to −20 °C and then 0.25 mL of a 1.6 M methyllithium solution in diethyl ether was added. The suspension of the lithium salt that formed upon warming the mixture to room temperature was transferred to a flask containing a solution of Mo$_2$(DAniF)$_3$(O$_2$CCH$_3$)$_2$ (406 mg, 0.400 mmol) in 15 mL of THF. The reaction mixture was stirred overnight and during this time the color changed from yellow to dark green. After the solvent was removed under reduced pressure, dichloromethane (20 mL) was added to the residue and the resulting solution was filtered. The volume of the filtrate was reduced to a volume of about 5 mL under vacuum and 40 mL hexanes were added to precipitate a green solid. After the solvent was decanted, the solid was washed with ethanol (2 × 15 mL) and hexanes (2 × 15 mL), and dried under vacuum. The solid was dissolved in 15 mL of THF and the solution was then layered with ethanol. Dark green crystals formed in 2 days.

Yield: 250 mg (60%). UV-vis, λ_{max} nm (ε, M^{-1} mol^{-1}): 390 (8.0 × 10^2), 500 (4.0 × 10^2), 750 (6.6 × 10^3). Anal. Calcd for $C_{100}H_{102}Cl_4Mo_4N_{14}O_{14}$ (**1·2CH$_2$Cl$_2$**): C, 53.39 H, 4.57 N, 8.72. Found: C, 53.63; H, 4.43; N, 8.91.

Preparation of [Mo$_2$(DAniF)$_3$]$_2${*trans*-C$_6$H$_2$(ONCH$_3$)$_2$}, 7. A similar procedure as that for **6** was used starting from 1,4-dihydroxyl-2,5-dimethylaminbenzene (33 mg, 0.20 mmol) and Mo$_2$(DAniF)$_3$(O$_2$CCH$_3$)$_2$ (406 mg, 0.400 mmol). Green crystals were obtained by diffusion of hexanes into a solution in a mixture of CH$_2$Cl$_2$ and acetone (1:1). Yield: 210 mg (50%). UV-vis, λ_{max} nm (ε, M^{-1} mol^{-1}): 383 (2.2 × 10^3), 511 (5.8 × 10^2), 779 (1.4 × 10^4). Anal. Calcd for $C_{98}H_{98}Mo_4N_{14}O_{14}$ (**1**): C, 56.37, H, 4.73 N, 9.39. Found: C, 56.35; H, 4.70; N, 9.35.

Crystal data for [Mo$_2$(DAniF)$_3$]$_2${*cis*-C$_6$H$_2$(ONCH$_3$)$_2$}, 6. Space group $P2_1/c$, a = 16.5233(18) Å, b = 24.371(3) Å, c = 29.569(3) Å, α = 90.00°, β = 106.110(2)°, γ = 90.00°, V = 11440(2) Å^3, T = 213(2) K, Z= 4, μ (λ = 0.71073 Å) = 0.501 mm^{-1}, ρ_{calc} = 1.417 Mg m^{-3}, 85184 reflections measured, 20356 unique, and 14709 ($I > 2\sigma(I)$) used in the calculations; $R1$ = 0.1029, w$R2$ = 0.1837. Interstitial solvent: C$_4$H$_4$O.

Crystal data for [Mo$_2$(DAniF)$_3$]$_2${*trans*-C$_6$H$_2$(ONCH$_3$)$_2$}, 7. Space group $P\bar{1}$, a = 11.345(4) Å, b = 16.008(6) Å, c = 16.851(6) Å, α = 70.111(7)°, β = 73.723(6)°, γ = 70.823(6)°, V = 2668.7(17) Å^3, T = 213(2) K, Z= 1, μ (λ = 0.71073 Å) = 0.727 mm^{-1}, ρ_{calc} = 1.505 Mg m^{-3}, 13608 reflections measured, 8886 unique, and 6214 ($I > 2\sigma(I)$) used in the calculations; $R1$ = 0.0874, w$R2$ = 0.1731. Interstitial solvent: CH$_2$Cl$_2$.

Details of the crystallographic data for **6** and **7** are in Table V.

Table V. X-ray Crystallographic Data for **6** and **7**.

Compound	$1 \cdot 5C_4H_8O$	$2 \cdot 4CH_2Cl_2$
Chemical formula	$C_{118}H_{138}Mo_4N_{14}O_{19}$	$C_{102}H_{106}Cl_8Mo_4N_{14}O_{14}$
Fw	2440.18	2419.37
Space group	$P2_1/c$(No. 14)	$P\bar{1}$ (No. 2)
a (Å)	16.5233(18)	11.345(4)
b (Å)	24.371(3)	16.008(6)
c (Å)	29.569(3)	16.851(6)
α(deg)	90.00	70.111(7)
β (deg)	106.110(2)	73.723(6)
γ (deg)	90.00	70.823(6)
V (Å^3)	11440(2)	2668.7(17)
Z	4	1
d_{calcd} (gcm^{-3})	1.417	1.505
μ (mm^{-1})	0.501	0.727
T (K)	213(2)	213 (2)
R1,[a] wR2[b]	0.1029, 0.1837	0.0874, 0.1731
R1,[a] wR2[b] (I > 2σ)	0.0599, 0.1392	0.0590, 0.1531

[a] $R1 = [\sum w(F_o - F_c)^2/\sum wF_o^2]^{1/2}$.

[b] $wR2 = [\sum [w(F_o^2 - F_c^2)^2]/ \sum w(F_o^2)^2]^{1/2}$, $w = 1/[\sigma^2(F_o^2) + (aP)^2 + bP]$, where $P = [\max(F_o^2,0) + 2(F_c^2)]/3$.

CHAPTER IV

CONCLUSIONS

Chapter II reported a series of molybdenum "dimers of dimers", formulated as $[Mo_2]L[Mo_2]$ where $[Mo_2]$ is a quadruply bonded Mo_2^{4+} core supported by ligands such as DAniF and L is the linker that connects the two $[Mo_2]$ units, have been synthesized and their properties have been investigated. Depending on the characteristics of the linkers involved, these dimers of dimers are divided into two categories: 1) heterometallic supramolecules that utilize complexes of metals other than Mo as a bridge to connect the two Mo_2 cores, and 2) tetranuclear species that have two $[Mo_2]$ moieties joined by organic linkers derived from zwitterionic quinones.

Electrochemical studies in Chapter III showed that the electronic communication between two bridged $[Mo_2]$ units is very weak for the dimers of dimers using inorganic metal complexes such as $ZnCl_2$, $Ni(acac)_2$ and $Rh_2(O_2CCH_3)_4$ as the bridging units, while it is exceptionally strong for the two dimers of dimers with organic quinone derivatives as the linking components. Rationales to these experimental results could be two fold: 1) since electronic coupling/communication reduces drastically with increasing length, compounds in the first category are expected to have very weak communication between the bridged $[Mo_2]$ units that are averaging almost 18 Å apart from each other, and 2) the linker ligands involved in the second category provide much more efficient metal (δ) to ligand (π) orbital overlap, which creates a pathway to facilitate electron flow between the two molybdenum redox centers with a much lower energy barrier and therefore enhances the electronic communication between the $[Mo_2]$ redox sites.

REFERENCES

1   (a) Blondin, G.; Gired, J.-J. *Chem. Rev.* **1990**, *90*, 1359 and references therein. (b) Gamelin, D. R.; Bominaar, E. L.; Kirk, M. L.; Wieghardt, K.; Solomon, E. I. *J. Am. Chem. Soc.* **1996**, *118*, 8085 and references therein.

2   (a) Creutz, C.; Taube, H. *J. Am. Chem. Soc.* **1969**, *91*, 3988. (b) Creutz, C.; Taube, H. *J. Am. Chem. Soc.* **1973**, *95*, 1086.

3   (a) Dogan, A.; Sarkar, B.; Klein, A.; Lissner, F.; Schleid, T.; Fiedler, J.; Zalis, S.; Jain, V. K.; Kaim, W. *Inorg. Chem*. **2004**, *43*, 5973. (b) Rigaut, S.; Olivier, C.; Costuas, K.; Choua, S.; Fadhel, O.; Massue, J.; Turek, P.; Saillard, J.-Y.; Dixneuf, P. H.; Touchard, D. *J. Am. Chem. Soc.* **2006**, *128*, 5859. (c) D'Alessandro, D. M.; Dinolfo, P. H.; Davies, M. S.; Hupp, J. T.; Keene, F. R. *Inorg. Chem*. **2006**, *45*, 3261.

4   Prassides, K. Ed. Mixed-valency Systems. Applications in Chemistry, Physics and Biology; Kluwer Academic Publishers: Dordrecht, The Netherlands, **1991**.

5   (a) Ward, M. D. *Chem. Soc. Rev.* **1995**, *34*, 121. (b) Astruc, D. *Acc. Chem. Res.* **1997**, *30*, 383. (c) McCleverty, J. A.; Ward, M. D. *Acc. Chem. Res.* **1998**, *31*, 842. (d) Li, Z.; Beatty, A. M.; Fehlner, T. P. *Inorg. Chem.* **2003**, *42*, 5707. (e) Biancardo, M.; Schwab, P. F.; Argazzi, R.; Bignozzi, C. A. *Inorg. Chem.* **2003**, *42*, 3966.

6   Robin, M. B.; Day, P. *Adv. Inorg. Chem. Radiochem*. **1967**, *10*, 357.

7   Hush, N. S. *Prog. Inorg. Chem*. **1967**, *8*, 391.

8   Cotton, F. A.; Murillo, C. A.; Walton, R. A. *Multiple Bonds between Metal Atoms, 3rd ed.*; Springer Science and Business Media, Inc. New York, **2005**.

9   (a) Chisholm, M. H.; Patmore, N. J. *Acc. Chem. Res.* **2007**, *39*, 19. (b) Burdzinski,

        G. T.; Ramnauth, R.; Chisholm, M. H.; Gustafson, T. L. *J. Am. Chem. Soc.* **2006**,

        128, 6776. (c) Chisholm, M. H.; Feil, F.; Hadad, C. M.; Patmore, N. J. *J. Am.*

        Chem. Soc. **2005**, *127*, 18150. (d) Barybin, M. V.; Chisholm, M. H.; Dalal, N. S.;

        Holovics, T. H.; Patmore, N. J.; Robinson, R. E.; Zipse, D. J. *J. Am. Chem. Soc.*

        2005, *127*, 15182. (e) Bursten, B. E.; Chisholm, M. H.; D'Acchioli, J. S. *Inorg.*

        Chem. **2005**, *44*, 5571. (f) Chisholm, M. H.; Pate, B. D.; Wilson, P. J.; Zaleski, J.

        M. *Chem. Commun.* **2002**, 1084. (g) Cayton, R. H.; Chisholm, M. H.; Huffman, J.

        C.; Lobkovsky, E. B. *J. Am. Chem. Soc.* **1991**, *113*, 8709.

10   (a) Cotton, F. A.; Donahue, J. P.; Lin, C.; Murillo, C. A. *Inorg. Chem.* **2001**, *40*,

        1234. (b) Cotton, F. A.; Donahue, J. P.; Murillo, C. A. *J. Am. Chem. Soc.* **2003**,

        125, 5436. (c) Cotton, F. A.; Donahue, P. J.; Murillo, C. A.; Pérez, L. M. *J. Am.*

        Chem. Soc. **2003**, *125*, 5486.

11   (a) Cotton, F. A.; Liu, C. Y.; Murillo, C. A.; Villagrán, D.; Wang, X. *J. Am.*

        Chem. Soc. **2003**, *125*, 13564. (b) Cotton, F. A.; Liu, C. Y.; Murillo, C. A.;

        Villagrán, D.; Wang, X. *J. Am. Chem. Soc.* **2004**, *126*, 14822.

12   Cotton, F. A.; Donahue, J. P.; Murillo, C. A. *Inorg. Chem.* **2001**, *40*, 2229.

13   (a) Cotton, F. A.; Liu, C. Y.; Murillo, C. A.; Wang, X. *Inorg. Chem.* **2003**, *42*,

        4619. (b) Cotton, F. A.; Dalal, N. S.; Liu, C. Y.; Murillo, C. A.; North J. M.;

        Wang, X. *J. Am. Chem. Soc.* **2003**, *125*, 12945.

14   Cotton, F. A.; Daniels, L. M.; Jordan IV, G. T.; Lin, C.; Murillo, C. A. *J. Am.*

        Chem. Soc. **1998**, *120*, 3398.

15   (a) Cotton, F. A.; Daniels, L. M.; Jordan IV, G. T.; Lin, C.; Murillo, C. A. *Inorg. Chem. Commun*. **1998**, 109. (b) Cotton, F. A.; Daniels, L. M.; Guimet, I.; Henning, R. W.; Jordan IV, G. T.; Lin, C.; Schultz, A. J.; Murillo, C. A. *J. Am. Chem. Soc*. **1998**, *120*, 12531.

16   Cotton, F. A.; Li, Z.; Liu, C. Y.; Murillo, C. A.; Zhao, Q. *Inorg. Chem*. **2006**, *45*, 6387.

17   Richardson, D. E.; Taube, H. *Inorg. Chem*. **1981**, *20*, 1278.

18   Cotton, F. A.; Liu, C. Y.; Murillo, C. A. *Inorg. Chem.* **2004**, *43*, 2267.

19   See for example: Lehn, J.-M. *Supramolecular Chemistry*; VCH Publishers: New York, 1995.

20   See for example: (a) Stang, P. J.; Olenyuk, B. *Acc. Chem. Res*. **1997**, *30*, 502. (b) Leininger, S.; Olenyuk, B.; Stang, P. J. *Chem. Rev*. **2000**, *100*, 853. (c) Schalley, C. A.; Lützen, A.; Albrecht, M. *Chem. Eur. J.* **2004**, *10*, 1072. (c) Swiegers, G. F.; Malefetse, T. J. *Chem. Rev.* **2000**, *100*, 3483.

21   See for example: (a) Fujita, M.; Tominaga, M.; Hori, A.; Therrien, B. *Acc. Chem. Res.* **2005**, 38, 371. (b) Fujita, M. *Chem. Soc. Rev.* **1998**, *27*, 417. (c) Fujita, M. *Acc.Chem. Res*. **1999**, *32*, 53. (d) Ruben, M.; Rojo, J.; Romero-Salguero, F. J.; Uppadine, L. H.; Lehn, J.-M. A*ngew Chem. Int. Ed.* **2004**, *43*, 3644. (e) Mirkin, C. A.; Holliday, B. J. *Angew. Chem. Int. Ed.* **2001**, *40*, 2022.

22   (a) Caulder, D.; Raymond, K. N. *Acc. Chem. Res*. **1999**, *32*, 975. (b) Klausmeyer, K. K.; Wilson, S. R.; Rauchfuss, T. B. *J. Am. Chem. Soc.* **1999**, *121*, 2705. (c) Evans, O. R.; Lin, W. *Acc. Chem. Res.* **2002**, *35*, 511. (d) Giananeschi, N. C.; Masar III, M. S.; Mirkin, C. A. *Acc. Chem. Res*. **2005**, *38*, 825.

23   (a) Launary, J.-P. *Chem. Soc. Rev.* **2001**, *30,* 386. (b) Liang, W.; Shores, M. P.;
        Bockrath, M.; Long, J. R.; Park, H. *Nature* **2002**, *417*, 725.

24   (a) Gatteschi, D.; Caneschi, A.; Pardi, L.; Sessoli, R. *Science* **1994**, *265*, 1054. (b)
        Zaleski, C. M.; Deperman, E. C.; Kampf, J. W.; Kirk, M. L.; Pecoraro, V. L.
        Angew. Chem. Int. Ed. **2004**, *43*, 3912. (c) Osa, S.; Kido, T.; Matsumoto, N.; Re,
        N.; Pochaba, A.; Mrozinski, J. *J. Am. Chem. Soc.* **2004**, *126*, 420.

25   (a) Ermer, O. *Adv. Mater.* **1991**, *3*, 608. (b) Aumüller, A.; Erk, P.; Klebe, G.;
        Hünig, S.; Von Schütz, J. U.; Werner, H. P. *Angew. Chem. Int. Ed. Engl.* **1986**,
        25, 740. (c) Campos-Fernández, C. S.; Galán-Mascarós, J. R.; Smucker, B. W.;
        Dunbar, K. R. *Eur. J. Inorg. Chem.* **2003**, 988.

26   (a) Shi, W.; Chen, X.-Y.; Zhao, B.; Yu, A.; Song, H.-B.; Cheng, P.; Wang, H.-G.;
        Liao, D.-Z.; Yan, S.-P. *Inorg. Chem.* **2006**, *45*, 3939.

27   (a) Sato, O.; Iyoda, T.; Fujishima, A.; Hashimoto, K. *Science* **1996**, *272*, 704. (b)
        Sato, O. *J. Photochem. Photobiol. C Photochem. Rev.* **2004**, *5*, 203.

28   (a) Cotton, F. A.; Lin, C.; Murillo, C. A. *Acc. Chem. Res.* **2001**, *34*, 759. (b)
        Cotton, F. A.; Lin, C.; Murillo, C. A. *Proc. Natl. Acad. Sci. U.S.A.* **2002**, *99*,
        4810. (c) Chisholm, M. H.; Macintosh, A. M. *Chem. Rev.* **2005**, *105*, 2949.

29   (a) Cotton, F. A.; Liu, C. Y.; Murillo, C. A.; Wang, X. *Inorg. Chem.* **2006**, *45*,
        2619.

30   Chisholm, M. H.; Cotton, F. A.; Daniels, L. M.; Folting, K.; Huffman, J. C.; Iyer,
        S. S.; Lin, C.; Macintosh, A. M.; Murillo, C. A. *J. Chem. Soc., Dalton Trans.*
        1999, *9*, 1387.

31   (a) Catalán, K. V.; Mindiola, D. J.; Ward, D. L.; Dunbar, K. R. *Inorg. Chem.*

1997, *36*, 2458. (b) Cotton, F. A.; Daniels, L. M.; Lin, C.; Murillo, C. A.; Yu, S-Y. *J. Chem. Soc., Dalton. Trans*. **2001**, *5*, 502.

32   Angaridis, P.; Berry, J. F.; Cotton, F. A.; Murillo, C. A.; Wang, X. *J. Am. Chem. Soc.* **2003**, *125*, 10327.

33   Yu, L.; Muthukumaran, K.; Sazanovich, I. V.; Kirmaier, C.; Hindin, E.; Diers, J. R.; Boyle, P. D.; Bocian, D. F.; Holten, D.; Lindsey, J. S. *Inorg. Chem.* **2003**, *42*, 6629.

34   Bera, J. K.; Bacsa, J.; Smucker, B. W.; Dunbar, K. R. *Eur. J. Inorg. Chem*. **2004**, *2*, 368.

35   In prior work, we had found that addition of $NaOCH_3$ to $Mo_2(DAniF)_3(O_2CCH_3)$ removes the acetate ligand, yielding CH_3COONa and a highly reactive compound $Mo_2(DAniF)_3(OCH_3)(CH_3OH)$. See: (a) Cotton, F. A.; Li, Z.; Liu, C. Y.; Murillo, C. A.; Villagrán, D. *Inorg. Chem*. **2006**, *45*, 767. (b) Cotton, F. A.; Li, Z.; Liu, C. Y.; Murillo, C. A. *Inorg. Chem.* **2006**, *45*, 9765.

36   When reaction of **2** and $Ni(acac)_2$ was carried out in THF, a red product was obtained. Crystals from CH_2Cl_2 and other solvents were poorly diffracting but unambiguously showed a zig-zag infinite chain with alternating dimetal species and single metal units having the formula {[*cis*-$Mo_2(DAniF)_2(O_2CC_5H_4N)_2][Ni(acac)_2]\}_n$. Crystallographic data for {[*cis*-$Mo_2(DAniF)_2(O_2CC_5H_4N)_2][Ni(acac)_2]\}_n$: space group = $P\bar{1}$, a =14.321(16), b = 14.331(16), c = 18.22(2) Å, α = 92.88(2), β = 110.84(2), γ = 97.32(2) (deg), V = 3447(7) $Å^3$.

37   Lin, C.; Protasiewics, J. D.; Smith, E. T.; Ren, T. *Inorg. Chem*. **1996**, *35*, 6422.

38   Cotton, F. A.; Mester, Z. C.; Webb, T. R. *Acta Crystallogr*. **1974**, *B30*, 2768.

39   Cotton, F. A.; Daniels, L. M.; Hillard, E. A.; Murillo, C. A. *Inorg. Chem.* **2002**, *41*, 2466.

40   Koh, Y.-B.; Christoph, G. G. *Inorg. Chem.* **1978**, *17*, 2590.

41   (a) Fine, D. A. *Inorg. Chem*. **1971**, *10*, 1825. (b) Hashagen, J. T.; Fackler, Jr., J. P. *J. Am. Chem. Soc*. **1965**, *87*, 2821.

42   Xu, G.-L.; Zou, G.; Ni, Y.-H.; DeRosa, M. C.; Crutchley, R. J.; Ren, T. *J. Am. Chem. Soc.* **2003**, *125,* 10057.

43   Rempel, G. A.; Legzdins, P.; Smith, H.; Wilkinson, G. *Inorg. Synth*. **1972**, *13*, 90.

44   *SMART V 5.05 Software for the CCD Detector System*; Bruker Analytical X-ray System, Inc.: Madison, WI, 1998.

45   *SAINT. Data Reduction Software. V 6.36A*; Bruker Analytical X-ray System, Inc.: Madison, WI, 2002.

46   *SADABS. Bruker/Siemens Area Detector Absorption and Other Corrections. V2.03*; Bruker Analytical X-ray System, Inc.: Madison, WI, 2002.

47   Sheldrick, G. M. *SHELXTL. V 6.12*; Bruker Analytical X-ray Systems, Inc.: Madison, WI, 2000.

48   (a) Creutz, C. *Prog. Inorg. Chem.* **1983**, *30*, 1. (b) Richardson, D. E.; Taube, H. *Coord. Chem. Rev*. **1984**, *60*, 107. (c) Chen, P.; Meyer, T. J. *Chem. Rev*. **1998**, *98*, 1439. (d) Ferretti, A.; Lami, A.; Murga, L. F.; Shehadi, I. A.; Ondrechen, M. J.; Villani, G. *J. Am. Chem. Soc.* **1999**, *121*, 2594. (e) Kaim, W.; Klein, A.; Gloeckle, M. *Acc. Chem. Res.* **2000**, *33*, 755. (f) Demadis, K. D.; Hartshorn, C. M.; Meyer, T. J. *Chem. Rev.* **2001**, *101*, 2655. (g) Brunschwig, B. S.; Creutz, C.; Sutin, N.

Chem. Soc. Rev. **2002**, *31*, 168. (h) Lau, V. C.; Berben, L. A.; Long, J. R. *J. Am. Chem. Soc.* **2002**, *124*, 9042.

49 (a) Tolbert, L. M.; Zhao, X.; Ding, Y.; Bottomley, L. A. *J. Am. Chem. Soc.* **1995**, *117*, 12891. (b) Sutter, J. P.; Grove, D. M.; Beley, M.; Collin, J. P.; Veldman, N.; Spek, A. L.; Sauvage, J. P.; Koten, G. V. *Angew. Chem., Int. Ed. Engl.*, **1994**, *33*, 1282.

50 (a) Joachim, C.; Launay, J.-P.; Woitellier, S. *Chem. Phys.* **1990**, *147*, 131. (b) Ribou, A.-C.; Launay, J.-P.; Sachtleben, M. L.; Li, H.; Spangler, C. W. *Inorg. Chem*. **1996**, *35*, 3735.

51 (a) Chisholm, M. H.; Patmore, N. J. *Dalton Trans.* **2006**, 3164. (b) Cotton, F. A.; Murillo, C. A.; Villagrán, D.; Yu, R. *J. Am. Chem. Soc*, **2006**, *128*, 3281.

52 Cotton, F. A.; Daniels, L. M.; Donahue, J. P.; Liu, C. Y.; Murillo, C. A. *Inorg. Chem*. **2002**, *41*, 1354.

53 (a) Siri, O; Braunstein, P.; Rohmer, M.-M.; Bénard, M.; Welter, R. *J. Am. Chem. Soc*, **2003**, *125*, 13793. (b) Yang, Q-Z.; Siri, O.; Braunstein, P. *Chem. Commun*. **2005**, 2660. (c) Siri, O; Braunstein, P. *Chem. Commun*. **2000**, 2223.

54 Chisholm, M. H.; Clark, R. J. H.; Gallucci, J.; Hadad, C. M.; Patmore, N. J. *J. Am. Chem. Soc.* **2004**, *126*, 8303.

55 (a) Yang, Q. Z.; Siri, O.; Braunstein, P. *ChemComm*, **2005**, 2660. (b) Siri, O.; Braunstein, P. *ChemComm*, **2000**, 2223.

56 Rolla N. Harger, *J. Am. Chem. Soc.,* **1924**, *46*, 2540.

VITA

Jiayi Jin was born in Jiaxing, China. He received his B.S. degree in Chemistry from University of Science and Technology of China in July 2005. He started his graduate study under the guidance of Prof. F. A. Cotton in May 2005 and received his M.S. degree in Chemistry from Texas A&M University in August 2007.

Jiayi Jin may be reached at Department of Chemistry, Texas A&M University, College Station, TX 77842 United States.

Email address: jjin@mail.chem.tamu.edu